Oceanography and Marine Biology: An Annual Review, 2019, **57**, 89–126

Taylor & Francis

ESTABLISHED AND EMERGING TECHNIQUES FOR CHARACTERISING THE FORMATION, STRUCTURE AND PERFORMANCE OF CALCIFIED STRUCTURES UNDER OCEAN ACIDIFICATION

SUSAN C. FITZER[1]‡*, VERA BIN SAN CHAN[2,3,4]‡, YUAN MENG[4], KANMANI CHANDRA RAJAN[4], MICHIO SUZUKI[5], CHRISTELLE NOT[6], TAKASHI TOYOFUKU[7], LAURA FALKENBERG[8,9], MARIA BYRNE[10,11], BEN P. HARVEY[12], PIERRE DE WIT[13], MAGGIE CUSACK[14], K. S. GAO[15], PAUL TAYLOR[16], SAM DUPONT[17], JASON M. HALL-SPENCER[18,19] & V. THIYAGARAJAN[4]*

[1]*Institute of Aquaculture, Faculty of Natural Sciences, University of Stirling, Pathfoot Building, Stirling, FK9 4LA, UK*
[2]*Department of Biological Sciences, Clemson University, Clemson, SC 29634 USA*
[3]*Ifremer, Physiologie Fonctionnelle des Organismes Marins UMR 6539 LEMAR (CNRS/UBO/IRD/Ifremer) Technopole Iroise - CS 10070 29280 Plouzane, France*
[4]*The Swire Institute of Marine Sciences and School of Biological Sciences, The University of Hong Kong, Hong Kong SAR*
[5]*Graduate School of Agricultural and Life Sciences, The University of Tokyo, Tokyo, Japan.*
[6]*Department of Earth Sciences, The University of Hong Kong, Hong Kong, China*
[7]*Institute for Extra-cutting-edge Science and Technology Avant-garde Research (X-star), Japan Agency of Marine Earth Science and Technology JAMSTEC, Department of Marine Biodiversity Research BioDive, Yokosuka, Kanagawa, Japan*
[8]*Norwegian Institute for Water Research NIVA, NIVA Region West, Thormøhlensgate 53 D5006 Bergen, Norway*
[9]*Simon F.S. Li Marine Science Laboratory, School of Life Sciences, The Chinese University of Hong Kong, Hong Kong*
[10]*School of Medical Sciences, University of Sydney, Sydney, New South Wales, Australia*
[11]*School of Life and Environmental Sciences, University of Sydney, Sydney, New South Wales, Australia*
[12]*Shimoda Marine Research Center, University of Tsukuba, 5-10-1 Shimoda Shizuoka 415-0025, Japan*
[13]*Department of Marine Sciences, University of Gothenburg, 45296 Stromstad, Sweden*
[14]*Division of Biological & Environmental Sciences, Faculty of Natural Sciences, University of Stirling, Cottrell Building, Stirling, FK9 4LA, UK*
[15]*The State Key Laboratory of Marine Environmental Science, Xiamen University, Xiamen, China*
[16]*Department of Earth Sciences, Natural History Museum, Cromwell Rd, London SW7 5BD, UK*
[17]*Department of Biological and Environmental Sciences, University of Gothenburg, 45178 Fiskebackskil, Sweden*
[18]*School of Biological and Marine Sciences, Plymouth University, Plymouth PL4 8AA, Devon, UK*
[19]*Shimoda Marine Research Centre, University of Tsukuba, Japan*

‡ *shared first-authorship*
**Corresponding author:* Susan C. Fitzer
e-mail: susan.fitzer@stir.ac.uk
**Corresponding author:* V. Thiyagarajan
e-mail: rajan@hku.hk

Abstract

Ocean acidification (OA) is the decline in seawater pH and saturation levels of calcium carbonate ($CaCO_3$) minerals that has led to concerns for calcifying organisms such as corals, oysters and mussels because of the adverse effects of OA on their biomineralisation, shells and skeletons. A range of cellular biology, geochemistry and materials science approaches have been used to explore biomineralisation. These techniques have revealed that responses to seawater acidification can be highly variable among species, yet the underlying mechanisms remain largely unresolved. To assess the impacts of global OA, researchers will need to apply a range of tools developed across disciplines, many of which are emerging and have not yet been used in this context. This review outlines techniques that could be applied to study OA-induced alterations in the mechanisms of biomineralisation and their ultimate effects on shells and skeletons. We illustrate how to characterise, quantify and monitor the process of biomineralisation in the context of global climate change and OA. We highlight the basic principles, as well as the advantages and disadvantages, of established, emerging and future techniques for OA researchers. A combination of these techniques will enable a holistic approach and better understanding of the potential impact of OA on biomineralisation and its consequences for marine calcifiers and associated ecosystems.

Introduction

The precipitation of minerals such as $CaCO_3$ for shells and skeletons using dissolved carbonate and calcium ions is commonly called *biomineralisation* (Doney et al. 2009). Marine organisms have been producing $CaCO_3$ biominerals since the Precambrian, and the resultant rich fossil record provides insight into the evolution of intricate, orderly and often beautiful structures (Wilkinson 1979). The composition of biominerals varies among taxa and, as the production of shell materials is dependent on the availability of mineral ion resources and on physiological conditions at the site of calcification (Wilbur 1964), mineral composition can reveal how organisms have interacted with environmental conditions over geological time to the present day.

Atmospheric CO_2 levels have increased at a faster rate during the Anthropocene than in any previous time in Earth's history, causing a rapid decline in seawater pH and lowering the amount of $CaCO_3$ minerals (Orr et al. 2005). Since concerns about ocean acidification (OA) were first highlighted (Feely et al. 2004, Raven et al. 2005) there has been a concerted international effort to understand its implications for marine life. It has become apparent that CO_2-driven acidification can lead to skeletal abnormalities and slower growth in many marine calcifiers (Hofmann et al. 2008, Vézina & Hoegh-Guldberg 2008, Wittmann & Pörtner 2013). Aragonite, calcite, vaterite (Wehrmeister et al. 2011) and amorphous $CaCO_3$, which is an important precursor of crystalline carbonate minerals (Addadi et al. 2003), are phases of $CaCO_3$ whose production may be modified by OA. Organisms can be affected by OA, as they need to maintain conditions that are chemically suitable for the process of calcification (supersaturated with calcium [Ca^{2+}] and carbonate [CO_3^{2-}]) or for preventing dissolution (saturation state $\Omega < 1$). Calcite is less susceptible to dissolution at lower pH values than aragonite unless it contains high levels of magnesium (Ries et al. 2009, Chan et al. 2012). Production of any form of $CaCO_3$ can be energetically expensive (Comeau et al. 2017a) and so the impact of OA on the production and maintenance of $CaCO_3$ structures are modulated by energy acquisition (Melzner et al. 2011) and may be due to CO_2-driven organism hypercapnia (Byrne et al. 2013).

To capture fully the impact of OA on biomineralisation, several key questions should be addressed. These include questions regarding the direct impact of OA on the process of biomineralisation itself, and also about the functional consequences of these changes on shells and skeletons. Resolving these issues requires multidisciplinary research ranging from omics to cell culture, from physiological mechanisms to ecology, and from materials science to crystallography. The complexity of the task is reflected in the plethora of techniques that have been used to investigate biomineralisation under OA conditions, including buoyant weight, total alkalinity anomality, total calcium content, annual estension, calcein labelling and the use of radio isotopes (Table 1). This diversity of approaches allows investigators to tackle different questions related to the impact of OA on the process of biomineralisation, although there is a need to understand how techniques compare when measuring similar processes (Schoepf et al. 2017). The selection and refinement of a technique depend upon scientific question and practical aspects related to the study question, experimental design and biological models (Figure 1).

Here, we review an array of techniques used to explore the consequences of rising global CO_2 levels on biomineralisation in marine organisms. We organise the techniques by the biological or mineralogical parameters of interest. We evaluate their advantages and disadvantages so that future work can more effectively measure the effects of OA on biomineralisation. We also highlight recent advances in the study of the effects of OA on biomineralisation and how interdisciplinary collaboration can advance the field.

Table 1 Summary of established techniques on growth and development to measure calcification and morphology under OA conditions

Technique	Measurements	Advantages	Disadvantages
Dyes— alizarin red and calcein	• Alizarin red stains; calcium-rich structures; a red/light purple colour • Calcein stains; calcium-rich structures; a fluorescent green colour	• Low cost, noninvasive • Track shell growth of living organisms during exposure to an experiment • Data comparable to published work • Dye location can be analysed with advanced characterisation methods	• Alizarin red also binds free Ca • Calcein also binds Ca^{2+}, Mg^{2+} and Zn^{2+} • Is not compatible with other fluorescence techniques, such as internal pH measurement • No mineral phase information
SEM	• High-resolution characterisation • Ultrastructures of minerals	• Low cost • Data are comparable • Provide structural information	• No mineral phase information
Buoyant weight	• Mineral content determined from the submerged weight of the organism	• Low cost • Noninvasive • More accurate than length or area measurements • Mineral density changes are reflected in measurement	• Seawater density varies when temperature and salinity change • Purpose-made setup needed
Radioactive isotopes	• ^{45}Ca incorporation rate • ^{14}C incorporation • Represents mineralisation process during an experiment	• More accurate than length or area measurements • Synthetic isotopes are specific to the study	• Invasive acid digestion of mineral samples are needed for scintillation measurement • Requires handling of radioactive substances
Total alkalinity anomaly technique	• Alkalinity reduction surrounding an organism	• Low cost • Accurate	• Incubation in individual organism required • Not suitable for long-term studies

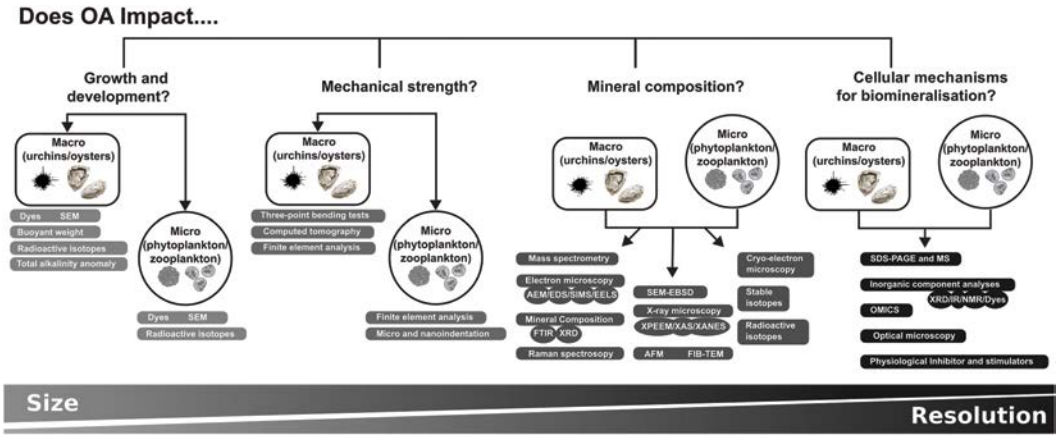

Figure 1 A schematic representation of analytical methods studying whole-animal growth and development, mechanical strength, mineral composition and cellular mechanisms of biomineralisation, which enables the answering of various levels of questions. These techniques can be strategically applied to macrobiota (e.g. urchin or oysters) or microbiota (e.g. phytoplankton or zooplankton). From left to right, the figure shows the techniques applicable to smaller-scale samples with increasing resolution. At a lower resolution, macrobiota can be measured in terms of various shell growth and development parameters and mechanical properties, while some approach has more limitations with microbiota. At a high resolution, microbiota and macrobiota can be studied for their shell structure and cellular mechanisms for biomineralisation.

Growth and development

When evaluating the impact of OA on biomineralisation, it is important to discriminate among methods measuring gross and net calcareous shell growth as the product of biomineralisation (Figure 2). The term *gross calcification* refers to the biologically controlled process of $CaCO_3$ production through the formation of $CaCO_3$ minerals from a supersaturated solution ($CaCO_3$ precipitation). In contrast, the term *net calcification* is the net effect of gross calcification and dissolution (Cyronak et al. 2016). $CaCO_3$ dissolution or decalcification is the dissolution of $CaCO_3$ minerals in an undersaturated solution. These processes combine to influence net calcification; for example, the upregulation in gross calcification rates of the limpet *Patella caerulea* helps to counteract faster shell dissolution rates (Rodolfo-Metalpa et al. 2011).

Dyes

A range of chemical dyes (e.g. alizarin red, calcein) are used to mark shells or exoskeletons to assess growth over time and have been used in OA studies to determine the impact on calcification in corals, coralline algae and bivalves (Rodolfo-Metalpa et al. 2011, Dickinson et al. 2012, Tambutté et al. 2012, Bradassi et al. 2013, Venn et al. 2013, Fitzer et al. 2014b, 2015b). Calcein labelling is often preferable because calcein was found to be better incorporated into foraminiferan calcite and emitted fluorescence more strongly than the other markers such as alizarin complexone, oxytetracycline and xylenol orange (Bernhard et al. 2004). Calcein has been applied in OA research to assess coralline algal, coral and mollusc growth during experiments (Dickinson et al. 2012, Bradassi et al. 2013, Venn et al. 2013, Fitzer et al. 2014b, 2015b). The techniques are low cost and less invasive than sacrificial shell sampling and the results are readily comparable.

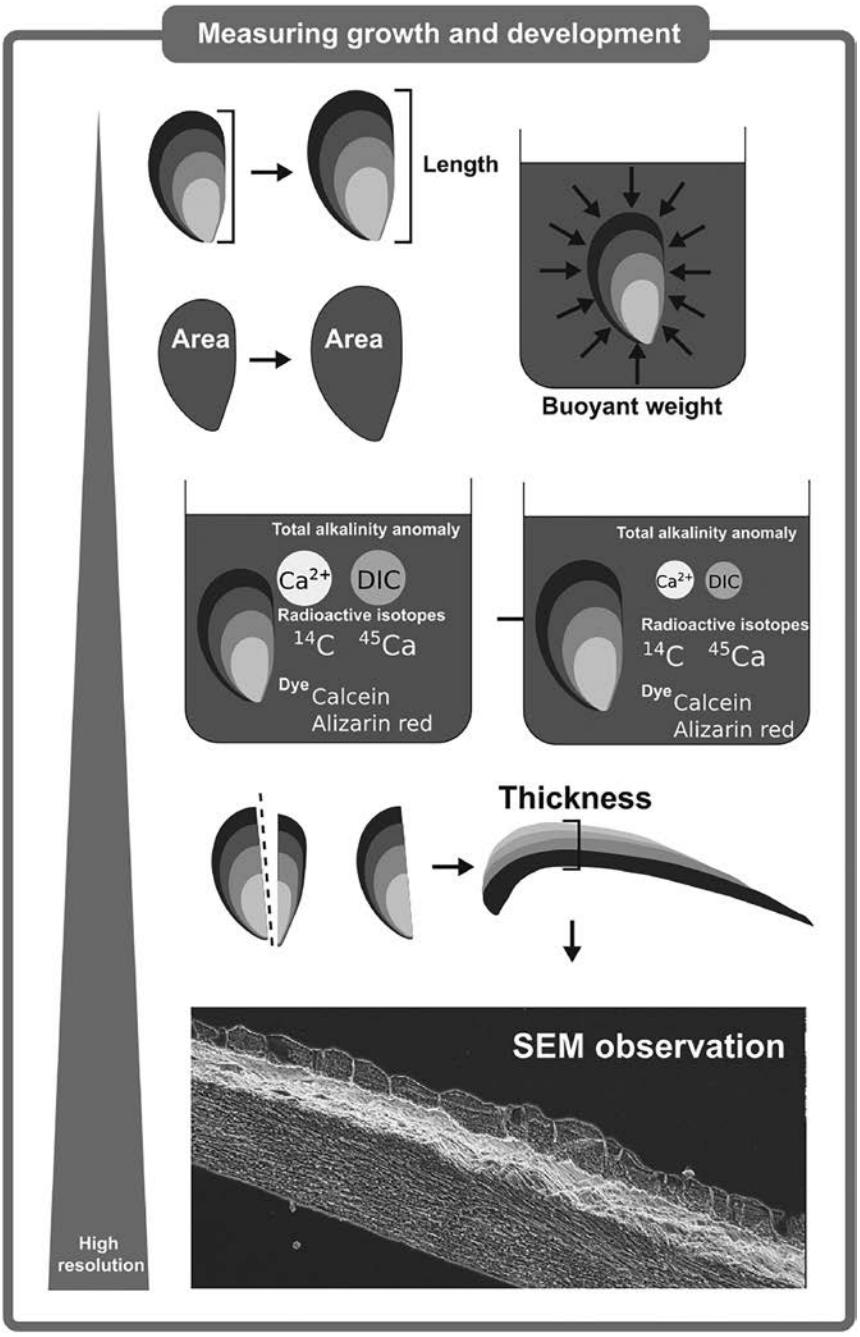

Figure 2 Schematic representation of techniques for measuring growth and development in biomineralising organisms. The tapering bar on the left indicates the changing level of resolution for each technique. From top to bottom, growth and development can be measured on whole shells and skeletons using techniques such as length and buoyant weight measurements. More sensitive techniques are represented in the middle for the use of dyes, radioactive isotopes and a total alkalinity anomaly technique. At the bottom, sectional surface of a shell at higher resolution can be visualised, and thickness can be measured using techniques such as SEM.

SEM

Abnormalities and morphology can be assessed by optical microscopy. However, scanning electron microscopy (SEM) is required for high-resolution characterisation of biomaterial microstructures and has been used to show modified skeletal phenotypes in a range of species grown under OA conditions (Riebesell et al. 2000, Orr et al. 2005, Iglesias-Rodriguez et al. 2008, Lombardi et al. 2015). The advantage of this approach includes the ability to assess shape and malformation in net growth, while the disadvantages include higher costs and an extended preparation time.

When evaluating net shell growth as the overall product of biomineralisation, one of the simplest and most widely used methods to approximate net calcification is shell and exoskeleton length, as it is both noninvasive and low cost. However, this approach can fail to reveal impacts on gross and net calcification that are not expressed in the overall structure of the skeleton. For example, OA can cause skeletal malformations that can be identified only by microscopy (Langdon et al. 2000, Reynaud et al. 2003, Langdon & Atkinson 2005, Gazeau et al. 2007, Cooper et al. 2008, Jokiel et al. 2008, Ries et al. 2009). This can be partly addressed by including morphometric parameters to resolve shapes, and thickness, for example using 3-dimensional measurements generated from computed tomography (Rühl et al. 2017). It is, therefore, important to consider the net growth of the whole shell or skeleton.

Skeletal growth assessed as annual extension rate (cm^2/yr) is commonly used to determine growth rates of calcareous red algae and corals (Marsh 1970), with recent research applying photogrammetric methods based on digital photography and advanced image-processing techniques for nondestructive measurements of area and volume (Mackenzie et al. 2014, Norzagaray-López et al. 2017). Densitometry using X-rays (Table 2) assesses the density of calcified structures (Carricart-Ganivet & Barnes 2007) and has been used to identify growth bands and to calculate growth rates of individuals or colonies (Cooper et al. 2008).

Buoyant weight

To monitor changes in mineral content, buoyant weight determined by immersion is frequently used (Davies 1989, Herler & Dirnwöber 2011). Correction for seawater salinity and temperature variation between measurements is necessary (Fang et al. 2013). The buoyant weight technique is noninvasive (Molina et al. 2005) and remains one of the most common techniques to determine net calcification rate in OA studies, especially in corals (Herler & Dirnwöber 2011). Such an approach has shown that an array of temperate corals (*Oculina arbuscular*), pencil urchins (*Eucidaris tribuloides*), hard clams (*Mercenaria mercenaria*), conchs (*Strombus alatus*), serpulid worms (*Hydroides crucigera*), periwinkles (*Littorina littorea*), bay scallops (*Argopecten irradians*), oysters (*Crassostrea virginica*), whelks (*Urosalpinx cinerea*) and soft clams (*Mya arenaria*) show mixed responses to CO_2-induced acidification, highlighting the complexity of biomineralisation responses (Ries et al. 2009).

Radioactive isotopes

Naturally occurring radioactive isotopes can be used to measure growth by spiking organisms with a radiotracer (Sabatier et al. 2012). Liquid scintillation counting is used to amplify the signal and quantify the amount or rate of ^{45}Ca being incorporated into the biomineral structure (Rodolfo-Metalpa et al. 2011, 2015). ^{45}C is a nonnatural radioactive isotope, so any changes in ^{45}Ca quantity represents shell material accretion or loss by the calcification process that occurs during the experiment, and prior calcification is not taken into account (Furla et al. 2000). Similarly, synthetic radioactive ^{14}C isotopes enable the measurement of carbon flux related to photosynthesis and calcification (Guo et al. 2009, Li et al. 2015). The ^{45}Ca technique has been used in OA research to determine the impact of increasing pCO_2 levels on cold-water corals, suggesting that calcification is not disrupted under OA (Rodolfo-Metalpa et al. 2015). Gross calcification rates have been quantified using ^{45}Ca in corals,

Table 2 Summary of emerging techniques on mechanical tests to investigate mechanical properties under OA conditions

Technique	Measurements	Advantages	Disadvantages
Three-point bending tests	• Elastic modulus • Fracture toughness	• Mimicking predatory attack • Simple operation • Low cost	• Requires a tailor-made device • Test samples are cut into a standard size for testing
CT	• Shell thickness • Shell volume • Shell density	• 3-dimensional visualisation of shell shape for morphometric analysis	• Hard to detect planktonic and larval samples (15–1000 μm per pixel) • Standard density calibrated with bone mineral density (BMD, in g/cm^3)
FEA	• Visualise structural weakness of a material • Provide a numerical model for material properties	• Links nanoindentation data to whole sample measurements • Takes shell shape changes into account • Data can be verified by mechanical tests	• Requires computational skills • Shape information requires simplified experimental data • FEA models need experimental verification
Microindentation	• Compressive force using 4-Vickers tip • Hardness • Elasticity modulus	• Broader Vickers tip is less localised than nanoindentation • Lower cost than nanoindentation • Provides microscale spatial resolution	• Localised measurement • Does not represent the shape and mechanical behaviour of the whole structure • Destructive to the sampling area of the specimen
Nanoindentation	• Compressive force using Berkovich tip • Hardness • Elasticity modulus	• Sharper Berkovich tip enables higher spatial refinement of measurements • Provides both hardness and elasticity data in one measurement	• Localised measurement • Does not represent the shape and mechanical behaviour of the whole structure • Destructive to the sampling area of the specimen

limpets, mussels, foraminifera, coccolithophores and oyster larvae (McEnery & Lee 1970, Erez 1978, Satoh et al. 2009, Rodolfo-Metalpa et al. 2011, 2015, Frieder et al. 2016). In contrast, ^{14}C has mainly been applied in unicellular organisms such as coccolithophores (Paasche 1963, Nimer & Merrett 1993, Gao et al. 2009), foraminifera (ter Kuile et al. 1989) and diatoms (Li et al. 2015). Advantages include the improved spatial resolution, taking into account material accretion during the incubation period. However, a major disadvantage of this technique is the destructive nature of sampling, unlike other techniques such as buoyant weight that are used to determine calcification rates.

Total alkalinity anomaly technique

Net calcification rate can be measured by determining the amount of $CaCO_3$ taken up by an organism (Gazeau et al. 2007). When an organism precipitates 1 mole of $CaCO_3$ it takes up 2 moles of HCO_3^-, thereby reducing the alkalinity of the surrounding seawater over the incubation period (Langdon et al. 2000, Langdon & Atkinson 2005, Gazeau et al. 2007). The total alkalinity anomaly technique has been used as an alternative to the buoyant weight method to determine net calcification rates in a range of calcifying organisms, including corals, mussels and oysters (Langdon et al. 2000, Langdon & Atkinson 2005, Gazeau et al. 2007). A recent study recommends that the technique is more suitable for shorter-term (e.g. day/night) incubations, whereas the buoyant weight method is suitable for longer-term studies

when resources are limited (Schoepf et al. 2017). Less frequently, calcium content has been determined directly using mass spectrometry as a proxy for calcification (Wood et al. 2008). Both the total alkalinity anomaly and the buoyant weight techniques are low cost and take into account skeleton malformations; however, there is variability between incubation methods. Promisingly, there is agreement in the results obtained from the various methods, with the major trend of a reduction in net biomineralisation under OA being shown by both techniques (Langdon et al. 2000, Langdon & Atkinson 2005, Gazeau et al. 2007).

Mechanical tests: Protective function or ability to survive

OA affects the gross and net calcification in many marine calcifiers, and therefore, it would be expected that OA would similarly affect the function of the shell or skeleton. Mechanical properties of shells/skeletons can be quantified by two parameters: (1) hardness (resistance to irreversible deformation) and (2) compressive strength (the force needed to induce cracking). These parameters can be used to evaluate the functional impacts of changes in biomineralisation under OA. For example, changes in these parameters have implications for the vulnerability of reef-forming species and associated ecosystems, as well as consequences for predator-prey interactions (Fu et al. 2016).

Three-point bending tests

As a classical, simplistic and low-cost approach to examine the mechanical features of brittle biomineral structures, three-point bending tests measure the flexural strength and modulus and commonly are used to define material properties in its ability to resist bending. Three-point bending tests have been applied to measure the stiffness of the ambital plates in sea urchins grown in OA, and it was found that there was no significant impact on the protective function of the exoskeleton (Collard et al. 2016). Devices made for the purpose of applying crushing tests, consisting of two supportive beams with appropriate span lengths and a loading beam, can be built according to the specific morphology of the biomineral sample (Guidetti & Mori 2005, Asnaghi et al. 2013). These tests provide relevant information to the protective function of the shell or exoskeleton. The flexural response to a three-point bending test device mimics the deformation response to predatory attack by fish (Guidetti & Mori 2005). This exoskeleton robustness test was applied in the OA study of a sea urchin and revealed increased pCO_2 reduced the defence of a sea urchin to the predator (Asnaghi et al. 2013). If samples are to be directly compared, it is essential to standardise the thickness and sectional area of the test material, which requires additional preparation time to ensure that the biomineral samples are cut to a standard size. The three-point bending tests have the advantage of being able to measure the whole structure mechanical response; their disadvantages are that it can be time consuming, as purpose-made devices may be required for unusually shaped shell structures.

Computed tomography

Computed tomography (CT) and micro-computed tomography (Micro-CT) are powerful, nondestructive techniques to evaluate biomineralised structures. Micro-CT allows 3D visualisation of X-ray image series generated by scanning with axial rotation in small steps. This method enables examination of internal structural features at fine spatial resolution (Li et al. 2016). A micro-CT data set allows a variety of quantifiable measurements, including thickness in terms of pixel distance, volume in terms of voxel counts and density in terms of brightness of each pixel at higher resolutions compared to CT (Fantazzini et al. 2015, Tambutté et al. 2015, Chatzinikolaou et al. 2017).

With these 3D geometric morphometrics and measurements, the growth rate, density and morphological changes due to OA can be investigated. Micro-CT has been applied in OA studies on gastropods (Chatzinikolaou et al. 2017), tubeworms (Li et al. 2014, 2016) and shrimp (deVries et al. 2016) to infer changes in the protective function of the exoskeletons. 3D-model visualisation also enables the analysis of density distribution to understand the engineering of calcareous structures.

Consequently, the presence of structurally vulnerable regions can be identified. Micro-CT analysis has been used in OA to determine the survival of coral through protective exoskeleton function (Tambutté et al. 2015). Exoskeleton porosity often represents shell protective function. In particular, the intertidal gastropods *Nassarius nitidus* and *Columbella rustica* exhibited density reduction in acidified conditions (Chatzinikolaou et al. 2017), while coral skeletons also showed an increased porosity at lower pH values through micro-CT (Fantazzini et al. 2015, Tambutté et al. 2015).

The spatial resolution of most medical micro-CT is sufficient to provide a good measurement for large calcifiers and typically have a resolution of 15–1000 μm per pixel. As a consequence, however, observation of marine plankton and larvae remains as a challenge. Another limitation of micro-CT is the detection sensitivity, which can generate false negatives through thin minerals where regions may appear as empty space in the 3D reconstruction. Therefore, it is important to verify the representative morphology by combining micro-CT with an SEM approach. All density measurements should be calibrated with a standard material that has a known bone mineral density (BMD, g/cm^3) in terms of calcium hydroxyapatite and its corresponding pixel intensity for each scan (Li et al. 2014). Because there are no commercially available standards for $CaCO_3$ calibration, density measurements are relative and has limited comparability with other studies.

Finite element analysis

The field of engineering and computational simulation can be applied creatively to understand structural impacts to biominerals caused by OA. In a simulation, any weakness in the architecture is highlighted and the loading capacity can be calculated from the shape and empirical data (Li et al. 2016). Therefore, the application of structural analysis can be performed when shapes and mechanical properties of the biological mineral are both known, providing a holistic picture of how well each calcified material functions as the protective or supportive structure.

The most widely applied numerical tool for computational simulation is finite element analysis (FEA) (Li et al. 2014, 2016). To solve a problem using FEA, the problem is divided into smaller and simpler parts, which are called *finite elements.* By assembling the solution of all finite elements mathematically, a total approximate solution of the large problem can be obtained. FEA enables the mechanical behaviours of complex biomineralised structures to be investigated accurately. The FEA can include the various experimental mechanical properties, such as elasticities of components of the shell structure, as well as simulate the effects of loading, such as the crushing forces associated with a predator attack.

With the diverse calcareous structures being produced by marine organisms, FEA can be applied to assess changes in mechanical performances due to morphological changes. For example, FEA has been applied to understand the mechanical response of a tubeworm under OA, combined with low salinity and warming treatments. This enabled the identification of the most vulnerable region of the tube and the highest risk of fracture failure under predatory attack (Li et al. 2014, 2016). This demonstrates that FEA can be developed as a biologically accurate model to determine the impact of OA on the protective function of calcareous shells and exoskeletons. However, a FEA model, especially when it is 2-dimensionally simplified (Ragazzola et al. 2012), often fails to account for heterogeneity, malformation and shape changes. Alternatively, 3-dimensional models are complex and require advanced computational efforts (Melbourne et al. 2015).

Microindentation and nanoindentation

Biominerals are composed of mineral crystals and an organic matrix framework. As a result, biogenic calcite has been reported to be 50%–70% harder than geological calcite (Kunitake et al. 2012, 2013). Due to the high heterogeneity in the morphology, structure and composition of mineralised shells and exoskeletons, hardness has been widely used as a comparable evaluation of mechanical properties (Beniash et al. 2010, Dickinson et al. 2012, Fitzer et al. 2015b) (Table 2).

The strength of biomineralised structures can be characterised by a crushing or compressive test in which a machine applies and reads compressive force versus displacement. The entire structure of specimens can be used to mimic a predatory attack (Byrne et al. 2014). However, biomineralised structures are typically not homogenous, and using a single point allows a better mechanical understanding of the shell property.

Two main methods can be used to understand the impact of OA on shell mechanical properties (Figure3): (1) microhardness tests can measure Vickers hardness, determined by the ratio of the force applied by the indenter and the surface area of the final indent (Beniash et al. 2010, Dickinson et al. 2012); and (2) nanoindentation, which can measure the hardness and elasticity in a single indent. With the development of a depth-sensing indenter, the hardness and elastic modulus (a measure of stiffness)

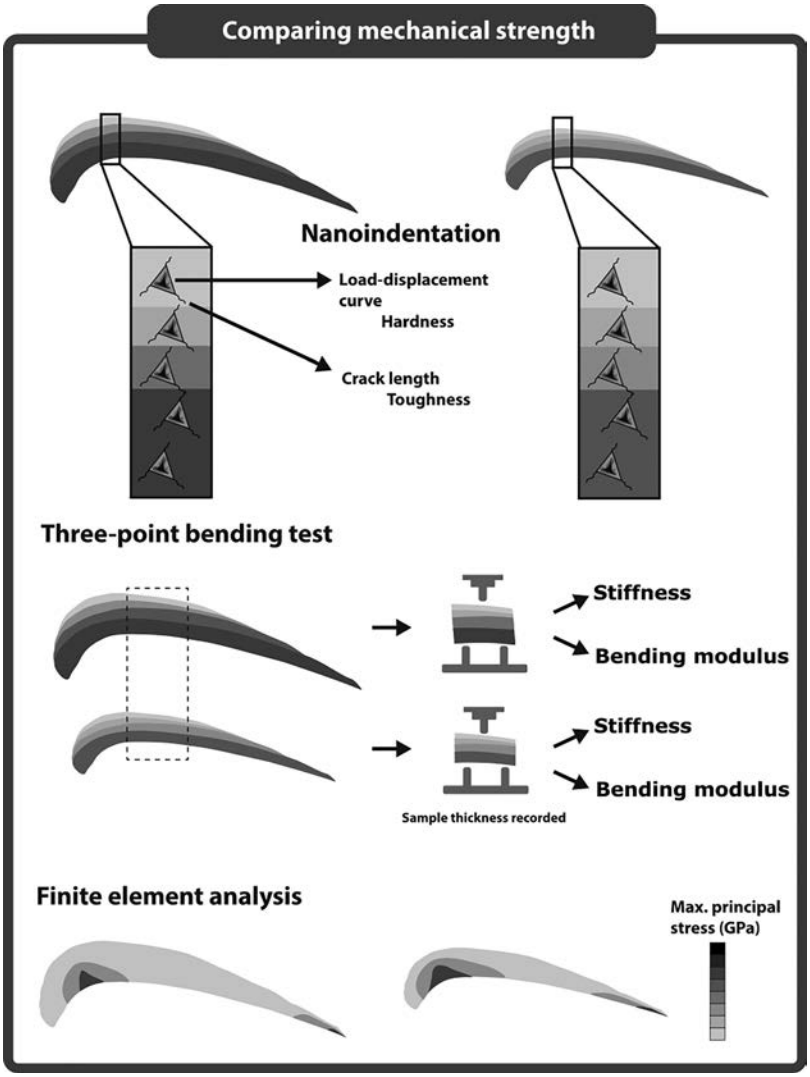

Figure 3 Schematic representation of techniques to compare the mechanical properties of biomineralising organisms. Nanoindentation and three-point bending are two highlighted techniques for assessing mechanical properties, including hardness, elasticity, fracture toughness and stiffness of biominerals. Microindentation and nanoindentation in the combination of CT and FEA project the impact of OA on the mechanical properties of shells and skeletons during predatory attacks.

measured in pascals (Pa) from each indentation can be obtained from the loading-unloading curve by using the Oliver–Pharr model (Oliver & Pharr 1992). This method enables the measurement of shell hardness and has been used to address how the protective function of several mollusc species grown under experimental OA might be affected (Beniash et al. 2010, Dickinson et al. 2012, Fitzer et al. 2015b). The results indicate no significant impact on microhardness in clams (Beniash et al. 2010) and oysters (Dickinson et al. 2012), but the microhardness in mussels increases (Fitzer et al. 2015b).

The advantage of nanoindentation is its precision at the nanometre scale. Nanoindentation enables spatial refinement, where the mechanical properties profile can be examined (Li et al. 2014). At finer spatial resolution, mechanical features can be associated with the different textures of the mineral (Goffredo et al. 2014). The influence of OA can be reflected in various mineralised layers or structures of the marine invertebrate shell. Nanoindentation enables substantial refinement, such as the hardness and modulus of the tubeworm from the exterior to the interior were mapped by nanoindentation to address questions about the protective function of the structure (Li et al. 2014, Fitzer et al. 2015b). The mechanical properties of the exterior to the interior portion of the tube were shown to decrease under OA compared to the middle portion of a tubeworm (Li et al. 2014). Researchers can analyse the same polished sample using SEM, allowing correlation between structural alteration and mechanical performance. This has been done for mussels (Fitzer et al. 2015b) and tubeworms (Chan et al. 2012, Li et al. 2014) grown in OA for extended periods of time, showing that OA-induced structural alteration may lead to deteriorations in mechanical performance. Both hardness tests have the disadvantage of requiring a highly polished sample surface (Perez-Huerta & Cusack 2009), and sample preparation can be both time-consuming and challenging (Milano et al. 2016).

In addition to hardness, the dimensions of the cracks generated around the indent can be used to determine the fracture toughness combined with the elasticity of the material as shown for bivalves grown under OA conditions (Beniash et al. 2010, Dickinson et al. 2012, Fitzer et al. 2015b). By measuring the lengths of cracks, the plane-strain fracture toughness can be calculated, applying the stress intensity factor (K) for a know compaction IC denoted as KIC. (Lawn et al. 1980, Anstis et al. 1981). However, it is difficult to define the local and bulk fracture behaviours by this technique, which makes it problematical to determine the accuracy of the fracture toughness values given by indentation (Kruzic et al. 2009). This technique has enabled the determination of the impact of OA on shell protective function. The fracture toughness of oyster shells and mussel shells was reduced (as measured by microhardness tests), which confirmed that the calcite shell became more brittle in OA conditions (Beniash et al. 2010, Dickinson et al. 2012, Fitzer et al. 2015b).

Mineral composition: Biomineralisation mechanisms to enable shell growth

Trace elements present in seawater are incorporated within the shell structure of calcifying organisms and several empirical relationships have been observed between the trace element-to-calcium ratio and environmental parameters of the surrounding water. For example, the Mg-to-Ca ratio of a shell is positively correlated with the temperature of the surrounding water (Nürnberg et al. 1996, Dwyer et al. 2013, Pérez-Huerta et al. 2008, Kamenos et al. 2013). Based on empirical and experimental calibration, several trace element-to-calcium ratios have been observed to reflect the environmental conditions. Trace element-to-calcium ratios, particularly Mg/Ca and Sr/Ca, have been widely used to examine the biomineralisation process (but note that biological activity can influence the elemental composition in the mineral, rather than recording the environmental conditions; see Weiner & Dove 2003). For example, OA has been shown to affect the trace element-to-calcium ratios in corals (Sinclair 2005), foraminifera (Elderfield et al. 1996, Keul et al. 2013, Not et al. 2018), ostracods (Dwyer et al. 2013) and tubeworms (Chan et al. 2015b), but not sea urchins (Byrne et al. 2014) (Table 3). For sea urchins grown under OA and warming from the juvenile to the adult stage, the Mg-Ca ratio was not affected by OA, but as expected, it was altered

Table 3 Summary of emerging techniques on mineral composition to investigate mechanical properties under OA conditions

Technique	Measurements	Advantages	Disadvantages
Elemental analysis			
ICP spectrometry	• Trace element-to-calcium ratios (e.g. Mg-Ca, Sr-Ca) • Analyse acid digested samples	• Quantitative • Data are comparable • Coupling with OES, MS or AES provides different sensitivity at various costs	• Destructive sample preparation • Requires elemental standards • More sensitive instruments are more expensive
LA	• Element-to-calcium ratios (e.g. Mg/Ca, Sr/Ca) • Analyse solid samples	• Spatial resolution • Less destructive than ICP approach • Data are comparable	• Spatial resolution of >5 μm, which is less than SIMS • Less sensitive than the ICP approach
AEM with EDS	• Element-to-calcium ratios (e.g. Mg-Ca, Sr-Ca) • Microanalysis provides a compositional map with spatial resolution	• Low cost and accessible • Spatial resolution • Nondestructive to specimen surface, so it can be followed by EBSD, LA-ICP-MS or nanoindentation	• Requires elemental standards • Detection level at 1000 ppm
AEM with WDS		• Moderate cost • Nanometre-scale resolution	• More expensive than AEM-EDS
Structured illumination microscopy		• Spatial resolution of SEM • Detection sensitivity of 1 ppm	• High cost • Destructive to the sampling area of the specimen
EELS		• 10 ppm detection limit • High-resolution compositional map	• High-cost • Require 10-nm-thick samples • Small region of interest
Mineral composition analyses			
FTIR	• Intensity ratio ($I_{max}\nu_2/I_{max}\nu_4$) between the absorption bands • Identifies the presence of aragonite or calcite	• Low cost • Provides a comparable measurement of ACC • Requires ~1 mg of mineral sample	• Semi-quantitative • No spatial resolution • Destructive

(*Continued*)

Table 3 (Continued) Summary of emerging techniques on mineral composition to investigate mechanical properties under OA conditions

Technique	Measurements	Advantages	Disadvantages
XRD	• Identifies the presence of aragonite or calcite	• Allows for quantification of calcite and aragonite ratios • Peak position suggests Mg content • Powdered sample can be acid-digested to provide elemental data	• Requires more powdered samples than FTIR • No spatial resolution • Destructive • Quantitative measurement requires the addition of CaF_2 as an internal standard
Raman spectroscopy	• Identifies the distribution of aragonite or calcite	• Spatial resolution • Area of calcite and aragonite is quantifiable • Specimen surface can be analysed by SEM and AEM methods for ultrastructure and elemental contents	• Requires sectional surfaces • Bleaching is necessary to remove organic contaminants • Limited spatial resolution
SEM-EBSD	• Identifies the distribution of calcite and aragonite • High-resolution crystallographic orientation data	• Allows visual comparison of mineral crystals • Provides quantifiable data on thickness of polymorphs • Spatial resolution	• Requires fine polishing • Sectional axis and plane of observation must be standardised • Moderate cost
XPEEM XAS XANES	• High-spatial resolution composition map • Localises and characterises ACC • Identify mineral phases	• High spatial resolution • Sample preparation enables SEM observation and SEM-EBSD characterisation	• High-cost • Requires fine polishing • Time-consuming
AFM	• Records force-distance curve • Visualises fine topographical features	• Nanometre resolution • Simple sample preparation • Possible to measure hydrated samples in electrolyte solution	• High-cost • Small area of interest • Time-consuming
FIB-TEM	• Fine spatial resolution • FIB prepares TEM sections	• Selective region of interest • High spatial resolution • Suitable for small samples	• High cost • Time-consuming • Small area of interest
Cryo-electron microscopy	• High-resolution study of biological sample after rapid freezing	• High resolution • Provides information on composition and crystallography	• High cost • Requires stabilising detergents for structure
Stable isotopes	• Detection of stable isotopes (e.g. δ13C, δ18O, 10B and δ11B)	• Data are comparable • Measures changes in metabolic activity in biomineralisation	• Destructive • Some proxies are not well established
Radioactive isotopes	• Calcification rate • Labelling with radioactive isotopes (e.g. ^{45}Ca and ^{14}C)	• Sensitive technique • Specific to experimental exposure	• Continual spiking of radiotracer required during incubation • Destructive

by temperature (Byrne et al. 2014). When exposed to OA, the Mg-Ca ratio increased in vermetid shells, suggesting a dissolution of aragonite and increase in calcite (Chan et al. 2012, Milazzo et al. 2014). Milazzo et al. (2014) applied inductively coupled plasma (ICP) optical emission spectrometry (ICP-OES) techniques to understand the impacts of OA on calcification as growth, and they suggested that under OA, shell dissolution will occur, with the potential to affect survival through weakened shell protection.

Mass spectrometry

A variety of methods are available to measure the elemental ratios of a biological mineral (Table 3). Basically, calcifying organisms can be measured in a solid phase using techniques such as X-ray fluorescence (XRF) or laser ablation (LA) or in dissolved phase after digestion using a range of ICP spectrometry. Because trace elements are measured within the mineral, several cleaning steps are required to remove organic matter and potential lithogenic contaminations (Martin & Lea 2002). Typically, analysis of a dissolved sample by ICP spectrometry requires the preparation of the shell or skeleton sample by acid digestion, fusion, or ash drying. Techniques for solution analyses include, ICP–optical emission spectrometry (OES), ICP–atomic emission spectroscopy (AES), ICP–mass spectrometry (MS) and multiple collector (MC) ICP-MS. The differences between these ICP spectrometry techniques are the increase in precision of the analyses, the higher resolution (and therefore lower detection limits) of elements up to isotopic measurement with MC-ICP-MS, whereas the disadvantages are the cost and maintenance of the equipment.

Electron microscopy AEM/EDS/SIMS/EELS

Spatial information of elemental distribution in the mineral provides valuable information to predict mechanical properties. Solid-sampling methods have been developed for ICP analysis for this purpose. Electrothermal-vaporisation (ETV) and LA are applied to generate vapour for characterisation. In combination with ICP-OES or ICP-MS, these techniques are suitable for analysis of a solid sample (Limbeck et al. 2017). However, LA-ICP-MS provides resolution of only >5 μm, while secondary ion mass spectrometry (SIMS) distinguishes submicrometre resolution (Becker et al. 2010). Although SIMS has a sensitive detection level of 1 ppm, the technique is not directly quantitative due to its dependence on a solid-state chemical standard, as well as the nonlinear and highly variable nature of the ionisation process of elements in SIMS (Williams 1985). In addition, secondary-ion mass spectrometry (SIMS) can be used to obtain depth profiles of mineral composition of shells (Jeffree et al. 1995). All these methods have an advantage of giving spatial information on the elemental distribution; the differences lie in the resolutions of ICP-MS, ICP-OES and SIMS. ICP-OES is already applied using acid digestion of collected individuals for determination of elemental ratios (Milazzo et al. 2014). The application of SIMS to OA research would enable the analysis of much smaller samples and to examine the response of individual calcifying organisms in terms of growth and survival (Eichner et al. 2017).

The spatial detection of trace elements on a bulk material surface can be achieved through electron microscopy (Müller et al. 2011). Analytical electron microscopy (AEM) with energy-dispersive X-ray spectrometry (EDS) and wavelength-dispersive X-ray spectroscopy (WDS) provides data at the nanometre scale (Newbury 1998). EDS offers an advantage of greater specimen area than the high-resolution method of electron energy loss spectrometry (EELS), which also requires a 10-nm-thick specimen to be prepared. Therefore, EDS is a more efficient and accessible AEM approach for OA research.

Notably, detection levels of AEM-EDS are around 1000 ppm, EELS 10 ppm and structured illumination microscopy 1 ppm. EDS and WDS both enable the microanalysis of biominerals and provide additional spatial information of the elemental profile. The cost of EDS is considerably

lower than WDS and has a high acquisition speed. In comparison, the spectral resolution of WDS is superior to that of EDS. These techniques have been applied to address the question of whether OA would have an impact on the calcification of shrimp and tubeworm skeletons, in order to understand the impact on exoskeleton critical function including protective defence against predators (Chan et al. 2012, Taylor et al. 2015). EDS was employed to determine magnesium content in the exoskeleton of shrimps grown under OA with the finding that increased calcium content with lowered pH resulted in a greater Mg/Ca ratio (Taylor et al. 2015). Mg/Ca as an environmental indicator of calcite has been suggested to increase as aragonite saturation decreases (Chan et al. 2012).

Taken together, there has been significant growth in a number of techniques available for quantifying elements present in liquid and solid materials. Some of the surface techniques, such as LA-ICP-MS, and other AEM techniques, such as SIMS, AEM-EDS and AEM-EELS, have different resolutions and sample preparation requirements, which should be considered in the context of experimental objectives. The recent development of MS analytic methods for bioimaging opens opportunities to investigate mineralising tissues at the biomolecule level (Becker et al. 2010). Complementing optical and electron microscopy techniques, as discussed in the following section, these tools will enable a better understanding of the mechanism of OA impacts on the processes involved in the production of biominerals. However, these techniques currently have the disadvantages of requiring sample specific standards for calibration, time-consuming sample preparation, observation confined to a tiny area of interest and the destructive nature of sample analysis.

Mineral composition analyses by FTIR and XRD

Mineral composition characterisation techniques target the comparison of mineral phases, elemental ratios and amorphous $CaCO_3$ to clarify the intricate process of biomineralisation (Figure 4). In the context of OA, it is important to understand the process of biomineralisation mechanisms to appreciate how continued growth will be possible under future environmental change.

Fourier-transform infrared (FTIR) spectra can be used to determine the relative quantity of amorphous $CaCO_3$ from an intensity ratio ($I_{max}\nu_2/I_{max}\nu_4$) between the absorption bands. The major disadvantage of the FTIR approach is its semi-quantitative nature; results can only be compared within the same experimental data set. This method has been adopted in OA research on a marine tube worm, where amorphous $CaCO_3$ content was found to be higher at low pH values (Chan et al. 2012, Leung et al. 2017). Chan et al. (2012) suggest that this result indicates the presence of an active shell repair mechanism when animals are counteracting shell weakening by OA. The advantage of FTIR is that it takes as little as 1 mg of mineral sample and thus may be applied to larval specimens.

The ratio of calcite and aragonite content, that has implications for the vulnerability of shells and skeletons to OA, can be quantified by X-ray diffraction (XRD). This is an advantage over FTIR, but XRD has its own drawback—namely, loss of spatial resolution due to the need for powdered samples. The XRD approach has been used to assess shell or exoskeleton growth under OA. Unless it contains large amounts of Mg, calcite is considered to be less susceptible to dissolution at lower pH values than aragonite (Ries et al. 2009, Chan et al. 2012). OA relevant changes in the thickness of the calcite and aragonite layers were first noted in mussels transplanted into low-pH environments (Hahn et al. 2012). Calcite-aragonite ratios have been shown to change under OA, leading to a thinner and more vulnerable aragonite layer in mussel shells (Fitzer et al. 2015a). The shell thickness index in comparison to the measured thickness of the aragonite or calcite layers uses the thickness, length, height and dry mass of the shell and is considered to produce a lower measurement error compared to direct measurement (Freeman & Byers 2006, Naddafi & Rudstam 2014, Fitzer et al. 2015a). The shell thickness index, in comparison to XRD, has the advantage of being nondestructuive to the sample, but it also has a disadvantage: a loss in spatial resolution.

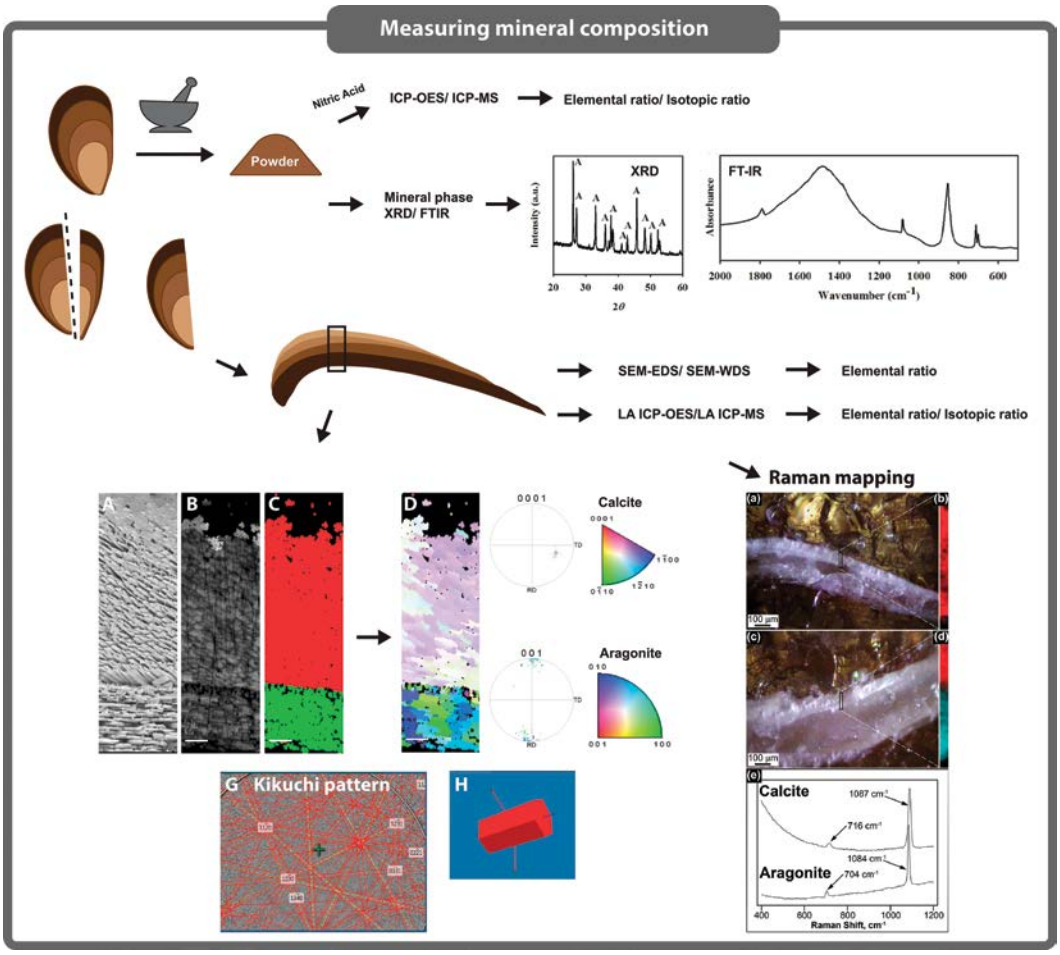

Figure 4 Schematic representation of highlighted techniques for characterising mineral composition in biomineralising organisms. Shell powder samples are digested prior to mass spectrometry characterisation (e.g. ICR-OES/ICP-MS) for determining elemental ratio or isotopic ratio. Sectional surface of the shell are inspected for elemental ratio mapping using electron microscopy techniques such as SEM-EDS or SEM-WDS; or using mass-spectrometry approaches by LA-ICP-MS or LA-ICP-OES. Additionally, a sample of shell powder provides mineral phase indentification using FTIR or XRD [figures modified from Chan et al. (2012)]. SEM-EBSD, SEM-WDS and Raman spectroscopy are highlighted as techniques to determine the mineral composition and crystallographic orientation in a mussel shell to determine the impacts on shell growth under OA as an alternative to techniques such as ICP-OES or ICP-MS to determine elemental or isotope ratios in biominerals. SEM-EBSD figure data taken from Fitzer et al. (2014a). Secondary electron images of the crystal structure from an etched (A) and polished (B) sample, the mineral composition can be seen in the phase map where calcite is shown in red and aragonite in green (C). The crystallographic orientation map (D), corresponding pole figures (E) and colour keys (F) are indicated for calcite and aragonite. EBSD uses Kikuchi patterns to identify the mineral phase (G) and the crystallographic orientation (H). Raman mapping figure modified from Chan et al. (2015b). Raman microscopy has been used to provide photomicrographs of younger (a) and older regions (c), of a juvenile tubeworm, phase maps indicate regions of aragonite only (b) and aragonite and calcite (d) in the tube. A Raman spectra (e) of aragonite and calcite has been measured in the same specimen (c).

Raman spectroscopy

Raman spectroscopy is a nondestructive technique that enables molecular bonds and mineralogical information to be precisely characterised at a submicron resolution. By illuminating a sample with a monochromatic laser beam, a Raman spectrum is generated that contains unique peaks that are diagnostic of mineral polymorphs due to their characteristic Raman shifts (Eisenstein et al. 2016). Structural components, such as calcite, aragonite and collagen, have been identified and mapped with resolution as fine as 1 μm (Eisenstein et al. 2016, Taylor et al. 2016). Advantages of Raman spectroscopy over other spectroscopic methods, such as FTIR, include the improved spatial resolution and the direct relevance of this method for biomineralisation, as well as the potential to examine samples in their native state (Eisenstein et al. 2016, Von Euw et al. 2017). This technique is considered a complementary method to FTIR, and is perhaps more suitable for OA studies. Raman microscope imaging has been applied to OA research to identify the mineral composition and polymorphic forms to assess rates of calcification under increasing pCO_2 in coralline algae and limpets (Kamenos et al. 2013, Langer et al. 2014). For instance, Raman mapping of the shells of limpets from a CO_2 vent demonstrated that the polymorph distribution pattern is maintained despite living at low pH (Langer et al. 2014). In coralline algae, although calcification continues under OA, Raman has identified disorder in the molecular position of the carbonate ions, which suggests a weakened skeletal structure (Kamenos et al. 2013). These applications were used to assess exoskeleton structural weaknesses, which can affect the protective function of the calcified structures under OA.

SEM-EBSD

Electron backscatter diffraction (EBSD) is widely used to determine the crystallographic orientation of biogenic minerals. EBSD provides additional information to precursory SEM imaging of shell dissolution or exoskeletal microstructure, as it allows for the examination of microstructure at the individual crystal level. The technique identifies Kikuchi patterns (Kikuchi 1928, Nishikawa & Kikuchi 1928) as scattered electrons are reflected as per Bragg's law from the crystal lattice onto a phosphorus screen. It was first used to observe the impact of OA on the shell ultrastructure of the mussel (*Mytilus galloprovincialis;* Hahn et al. 2012) and was further applied across a broad range of species, including argonauts (Wolfe et al. 2013) and corals (Hennige et al. 2015). The effects on crystalline structure identified using this technique in OA research have been used to address the question of how changes in seawater environment can affect the orderly arrangement of shell or exoskeleton structures, which has an implication for the animal's ability to survive.

X-ray microscopy XPEEM: XAS and XANES

An alternative emerging technique for determining the mineral composition of marine skeletons is high-spatial resolution synchrotron X-ray photo emission electron microscopy (XPEEM) combined with X-ray absorption spectroscopy (XAS) (Fitzer et al. 2016). The benefits of the XPEEM and XAS over SEM is the high level of spatial resolution, as well as the fact that it can detect without the need for an energy filter by measuring the secondary electrons yield as a function of photon energy. This technique can be applied alongside EBSD to identify mineral phases throughout the shell structure (Fitzer et al. 2016). X-ray absorption near edge structure (XANES) and XPEEM techniques use the principles of X-ray absorption fine structure (XAFS), which interpret the scattering of photoelectrons emitted from an absorbing atom in a structure when excited by high-energy photons (Politi et al. 2008, Fitzer et al. 2016). XANES has been used as a tool to examine the phase transformation mechanisms of amorphous $CaCO_3$ into calcite, particularly in sea urchin larval spicules (Politi et al. 2006, 2008, Gong et al. 2012). Recently, XPEEM combined with XAS has been used as a tool to examine amorphous $CaCO_3$ in mussels reared under OA conditions (Fitzer et al. 2016) showing

more induced amorphous $CaCO_3$ with less crystallographic control over shell formation. This technique was applied to address the question of OA impact on biomineralisation and shell repair to determine the protective function of the shell under changing environments (Fitzer et al. 2016). The technique requires the embedding and fine-polishing of samples, similar to SEM-EBSD preparation (Politi et al. 2008, Perez-Huerta & Cusack 2009, Fitzer et al. 2016). XANES and XPEEM have the advantage of providing high spatial resolution to locate amorphous $CaCO_3$ embedded within the shell structure when applied in combination with SEM techniques (Politi et al. 2008). Disadvantages include the high instrumentation cost and lengthy sample preparation time.

AFM

Atomic force microscopy (AFM) provides atomic resolution analysis of material properties. As a type of scanning probe microscopy, AFM scans and interacts with a sample directly using a tip that is connected to a cantilever spring. The vertical deflection and the force-distance curve are recorded by a piezoelectric translator (Butt et al. 2005). In tapping mode, AFM generates fine topographical images with nanometre resolution. The time-dependent relationship between applied pressure (stress) and deformation (strain) represents viscoelastic properties (Butt et al. 1995) that enable the measurement of local mechanical properties.

Easy sample preparation and high resolution are the major advantages of using AFM over conventional microscopy methods (Butt et al. 1995). The typically small interacting surface for AFM must be smooth and homogeneous, requiring polished and etched surfaces similar to EBSD sample preparation (Dalbeck et al. 2011). Therefore, AFM complements the observations of SEM-EBSD analysis, which can provide high-resolution textural data for OA studies (Dalbeck et al. 2011). AFM performed in the presence of an electrolyte solution is possible (Butt et al. 1995), and therefore enabling better biological relevance. In order to obtain comparable regions of interest, correlative SEM or light microscopy data are often helpful to effectively navigate at AFM resolution (Sikes et al. 2000). AFM has yet to be applied to determine the impact of OA on biomineralisation. Once applied, this technique will provide a correlation with EBSD data to address the question of biomineralisation mechanisms in shell growth (and hence survival).

FIB-TEM

The finest biological observations have been achieved via transmission electron microscopy (TEM), providing resolutions of nanometres down to below 1 angstrom (Nellist et al. 2004), exceeding superresolution microscopy. In addition, TEM is an important characterisation tool that collects XRD with a micrograph, enabling the subcellular features and location of crystals to be analysed together. A nanofabrication technique using the focussed ion beam (FIB) system has emerged as a powerful tool for precise TEM specimen preparation, where milling and cutting of a sample is performed inside an SEM or scanning ion microscopy (SIM) (Titze & Genoud 2016). This preparation approach overcomes the technical challenges of manual preparation of ultrathin TEM sections, with the localisation of the region of interest, and reduces the risks of sample loss (Chan et al. 2017).

Suzuki et al. (2011) revealed the details of five microstructures in the limpet shell using FIB-TEM. The FIB technique was used to separate each microstructure in cross section to determine crystal morphology and orientation. The FIB technique is powerful in handling tiny larval or juvenile shells (Yokoo et al. 2011, Chan et al. 2015a, 2017), and reduces costs of analysis time for TEM on samples with poor orientation or an unfocussed area of interest. FIB-TEM ensures a consistent cutting angle at the nanoscale, so providing comparable observation of a larger number of experimental samples.

Depending on institutional resources, fine spatial resolution, long-hour procedures performed using FIB-TEM can be costly in a centralised facility. In summary, FIB-TEM is currently a qualitative observational method, but it has the potential to be applied in a more quantitative setting.

Cryo-electron microscopy

In cryo-electron microscopy, biological samples can be visualised by a freeze fracture process that is achieved by rapid freezing of fixed tissue samples by vitrification (Alfredsson 2005). A hydrated sample that is close to the native state can be observed in high resolution without the requirement of destructive conventional preparation procedures for SEM and TEM (Levi-Kalisman et al. 2001, Khalifa et al. 2016, Thompson et al. 2016). Electron microscopy also enables XRD characterisation essential for identification of minerals. Ice from humidity in the environment can contaminate the sample; therefore, samples must be prepared after vitrification (Thompson et al. 2016). Technical disadvantages associated with cryomethods include the need for stabilising detergents for structure (Singh & Sigworth 2015) which, in addition to its high cost, will make the application of this technique challenging for large-scale OA experiments.

Stable isotopes

Biogenic stable isotopes have been used extensively to reconstruct the paleaoclimates in terms of temperature, pH and salinity (Lear et al. 2000, Parkinson et al. 2005, Ghosh et al. 2006, McConnaughey & Gillikin 2008, Martin et al. 2016, Stewart et al. 2016). They can also be used to understand biomineralisation mechanisms of ion transport at the site of calcification (Furla et al. 2000, Rae et al. 2011, Allen et al. 2012, Allison et al. 2014). The detection of Mg, Sr and Ca, the detection of the isotopes, $\delta^{13}C$, $\delta^{18}O$, ^{10}B and $\delta^{11}B$ requires acid digestion prior to mass spectrometry analyses (Krief et al. 2010). Here, we list some of the target isotopes that have promise for OA research.

Quantification of isotopic elements can be applied to detect the consequence of stress on calcification pathways (Rae et al. 2011, Allison et al. 2014, Stewart et al. 2016). Brachiopods, in particular, form their exoskeletons in good isotopic equilibrium with the seawater (Parkinson et al. 2005). Because pH is dependent on two boron species: boric acid ($B(OH)_3$) and the borate ion ($B(OH)_4^-$) (Hemming & Hanson 1992, Stewart et al. 2016, Zhang et al. 2017), the species of boron isotopes found in shells represents the dissolved inorganic carbon (DIC) chemistry of the calcification fluid (Allison et al. 2014). Stable isotope techniques have been applied in OA research to understand the mechanisms of biomineralisation—specifically, whether material is laid down under control by the organism, irrespective of the seawater isotopes (Krief et al. 2010). For example, seawater pH affects the skeletal $\delta^{13}C$ and $\delta^{18}O$ in corals, but there is an offset in the $\delta^{11}B$ between the calcified material and that of seawater, suggesting control of biomineralisation by ion-transport enzymes (Krief et al. 2010). This technique addresses the question of calcification mechanism change under OA and whether there is a reduced metabolic incorporation of isotopes through enzyme control (hence reduced growth and survival under OA). The influence of carbonate ion concentration on $\delta^{13}C$ and $\delta^{18}O$ is still being explored, particularly in foraminifera (Spero et al. 1997).

Isotopic approaches have the disadvantage of requiring a relatively large amount (~2 mg) of biogenic $CaCO_3$ powder. Sample preparation with micromilling is time consuming and can be technically challenging, especially when investigating different polymorphs and seasonal growth bands in smaller specimens (Stewart et al. 2016). Advances in stable isotope techniques will consist of improved ways of separating organics from biominerals, micromilling samples for biomineral powder, and LA methods that increase spatial resolution of measurements (Fietzke et al. 2010, Wall et al. 2016).

Radioactive isotopes

In addition to using ^{45}Ca for estimation of calcification, radioactive isotopes can contribute to a mechanistic understanding of the calcification process. Furla et al. (2000) used a double radioactive isotope experimental design ($H^{14}CO_3$ and ^{45}Ca) to show inorganic carbon transport. Comprehensive

measurement of both the DIC species and Ca for calcification was accomplished in terms of net radioactivity by ^{14}Ca and ^{45}Ca (Furla et al. 2000). These data also unraveled the carbonate-concentrating mechanisms within coral cells (Furla et al. 2000).

The use of radioactive isotopes (^{45}Ca, ^{14}C) is specific and sensitive to experimental conditions. Moreover, the maintenance of radioactive substances can be challenging. Before adopting the use of radioactive isotopes within an experimental culture, a protocol must be optimised to label specimens adequately and avoid contamination. Therefore, even though the approach is quite well established in environmental geochemistry (Parkinson et al. 2005, Ghosh et al. 2006, McConnaughey & Gillikin 2008), the disadvantages of requiring continual radioactive tracer application and the destructive nature of the sample digestion by acid mean that it has yet to be applied more widely in OA studies (Furla et al. 2000).

Cellular biomineralisation mechanisms

The processes by which organisms control the substrate for calcification are complex and can occur internally within tissues, or outside the organism, but both need to modify the seawater chemistry for calcification to take place (Roleda et al. 2012). It is thought that HCO_3^- is the choice of substrate for biomineralisation, which can be taken directly from seawater or metabolised from CO_2 (Roleda et al. 2012). The mechanisms revolve around producing an abundance of ions and the right conditions to favour the precipitation of $CaCO_3$ from available Ca^{2+} and CO_3^{2-} (Roleda et al. 2012). An understanding of biomineralisation mechanisms under forecasted OA conditions will require the use of a wide range of techniques (Figure 5), but it also works at different levels, from genes to organisms and ecosystems. This can be achieved by taking advantage of established techniques from other disciplines. For example, methods to culture larval sea urchin primary mesenchyme cells facilitate the study of the calcification process *in vitro* (Basse et al. 2015). Identifying and evaluating the roles of organic molecules in shells is a major topic in biomineralisation as the mechanical properties of shells are highly influenced by their 1% content of organic components. In the context of OA impacts on marine calcifiers, the response of organic molecules provides insight into cellular mechanisms for the ability to reproduce and develop and can be applied to all marine organisms, irrespective of size (Figure 1, schematic of question versus scale). Mechanisms of biomineralisation are largely unresolved and vary from species to species.

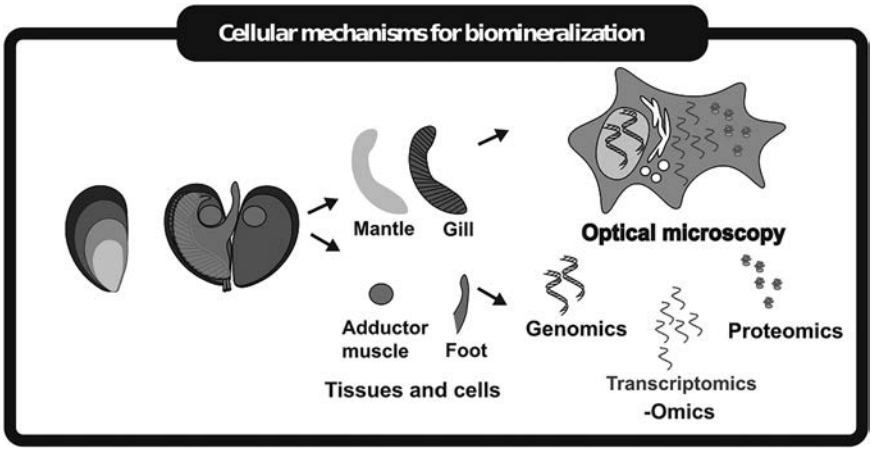

Figure 5 Schematic representation of techniques to examine the cellular mechanism of biomineralisation. Techniques with omics and optical microscopy are established techniques that could be applied to various tissues and cells to determine the impact of OA on molecular biomineralisation.

SDS-PAGE and MS

Shell protein extraction is achieved by recovering the protein from decalcified shell. Sodium dodecyl sulfate-polyacrylamide gel electrophoresis (SDS-PAGE), or 2-dimensional gel electrophoresis enables a comparison of protein profiles. In addition, mass spectrometry (MS) enables the identification of proteins from available databases. As marine organisms studied in OA research are usually not model-organisms, protein identification is challenging. Protein purification, protein sequencing and protein digestion may be required in the identification process (Marxen et al. 2003, Suzuki et al. 2004). When a large protein (more than 30 kDa) needs to be identified, cloning methods can be used to recover the nucleotide sequence for deduction of the protein sequence (Miyamoto et al. 1996, Samata et al. 1999, Suzuki et al. 2009, 2011). Many genome and transcriptome databases of calcifying invertebrates generated by next generation sequencing are also available as open resources (Takeuchi et al. 2012, Zhang et al. 2012).

MS is also a promising technique to understand shell proteins (Table 4). The MS/MS spectra of peptides allow the determination of amino acid sequence without a need for a protein sequencer, and MS/MS has become a low-cost and high-throughput technique. The combination of MS/MS and databases from next-generation sequencing is dramatically increasing the efficiency of protein identification (Joubert et al. 2010, Marie et al. 2010, 2011). The potential disadvantage of generating big data from the high-throughput process is covered in more detail in the next section. These techniques have been applied to show the proteome responses of invertebrates grown in OA conditions. For example, the shell matrix proteins of the larval pacific oyster (*Magallana gigas*) were observed to decrease under OA (Harney et al. 2016).

SDS-PAGE and MS offer advantages of low-cost and (in the case of MS) high-throughput protein identification to understand why physiological responses may be influenced by OA. The disadvantages of these techniques include time-consuming sample preparation to extract and purify proteins for analysis and production of big data, which can be difficult to interpret.

Insoluble organic component analyses using XRD, IR and pyrolysis NMR, and dyes

Insoluble organic components in the shell, such as chitin, are an essential polysaccharide that connects organic matrices and the initial deposition of the mineral (Nakayama et al. 2013); it serves as a scaffold for organic materials during the deposition of minerals. For example, the molluscan periostracum is made of chitin and it serves as a waterproof layer of a calcification compartment. Chitin is commonly found in the forms of α and β-chitin. Crustaceans use α-chitin in their exoskeletons and molluscs use β-chitin in their shells, as such, chitin is an essential additive to greatly improve the mechanical properties of biomaterials. Due to the insoluble and organic nature of chitin, the impact of OA on chitin content is currently unknown. There are many techniques to identify chitin, including XRD (Weiner & Traub 1980, Levi-Kalisman et al. 2001, Falini et al. 2003), infrared (IR) spectroscopy in the fingerprinting region (700–1800 cm^{-1}) (Pearson et al. 1960) and nuclear magnetic resonance (NMR) or MS detection of the glucosamine hydrochloride after hydrolysis (Nakayama et al. 2013). The analysis of pyrolysis (thermal decomposition of materials in a vacuum) gas chromatography–mass spectrometry (GC-MS) is able to identify characteristic chitin decomposition markers (Furuhashi et al. 2009). However, many other contaminants (such as proteins) produce a complex of unknown peaks that make the identification of chitin in biominerals difficult and, in the case of insufficient crystallinity, a clear diffraction pattern may be hard to obtain. Recently, a colorimetric assay of chitin has been developed to quantify chitin (Katano et al. 2016). The workers found that upon complete hydrolysis of chitin in strong acid (5M HCl), characterisation of depolymerised glucosamine is possible using colorimetry at the absorbance maximum at 750 nm. The method

Table 4 Summary of emerging techniques on cellular biomineralisation mechanisms to investigate mechanical properties under OA conditions

Technique	References	Measurements	Advantages	Disadvantages
SDS-PAGE and MS	Miyamoto et al. (1996), Samata et al. (1999), Marxen et al. (2003), Suzuki et al. (2004), (2009), (2011)	• Characterises shell proteins	• Established protocol for protein identification • Low cost and high throughput of samples	• Sensitivity insufficient to detect shell proteins occurring at low quantity • Protein extraction and purification is time consuming • Difficult to interpret sequences from nonmodel marine organisms
Insoluble organic component analysis using XRD	Weiner and Traub (1980), Levi-Kalisman et al. (2001), Falini et al. (2003)	• Characteristic spectroscopy correlated to chitin	• Provides evidence on the presence of chitin • Analyses insoluble solid samples	• Destructive • Sufficient sample is hard to obtain • Information has poor relevance to the cells and tissue associate with chitin
Insoluble organic component analysis using IR spectroscopy	Pearson et al. (1960), Suzuki et al. (2007)			
Pyrolysis NMR GC-MS	Furuhashi et al. (2009), Nakayama et al. (2013)	• Detects decomposition product of chitin after chitinase action	• Analyses the digested products • Digested product peaks can be quantified and compared	• Requires chemical standards of digested products • Protocol optimisation can be time-consuming
Colorimetric assay for acid hydrolysate of chitin	Katano et al. (2016)	• Detects decomposition product of chitin after acid hydrolysis	• Low cost • Quantitative • Simple protocol	• Destructive • Cannot distinguish forms of chitin • Spatial information is lost
Calcofluor-white Wheat-germ agglutinin (WGA)	Shillito et al. (1995)	• Visualises chitin in relation to cells and tissues	• Nondestructive to tissues and cells • Low cost • Commercially available	• Also binds to cellulose • Also binds to N-acetyl-D-glucosamine and sialic acid
CBD-GFP	Weiss and Schönitzer (2006), Nudelman (2007), Chan et al. (2018)		• Nondestructive to tissues and cells • Specific to chitin	• Requires a time-consuming bioengineering approach to express and purify CBD-GFP

(*Continued*)

Table 4 (Continued) Summary of emerging techniques on cellular biomineralisation mechanisms to investigate mechanical properties under OA conditions

Technique	References	Measurements	Advantages	Disadvantages
OMICS – transcriptomics	Takeuchi et al. (2012), Zhang et al. (2012)	• mRNA of expressed genes	• Assesses the molecular pathways of the organism from expressed genes or proteins • Provides a whole physiological picture	• mRNA presence may not represent protein activities • Tissue-specific response • Costly • Identification of transcripts in a nonmodel marine species is difficult
OMICS – proteomics	Dineshram et al. (2015)	• Total protein profile		• Shell proteins occurring at low quantity of 5% • A high-sensitivity method like iTRAQ is very costly • Identification of protein in a nonmodel marine species is difficult
Cellular pH imaging	Venn et al. (2011), Stumpp et al. (2012), Tambutté et al. (2015), Chan et al. (2017), Toyofuku et al. (2017)	• Intracellular pH indicated by a pH sensitive ratiometric probe • Visualises the sites of biomineralisation	• Examines living organisms • High swpatial resolution	• Not well established and requires optimisation and customisation • Ratiometric pH probes require calibration
Physiological inhibitors and stimulators	Toyofuku et al. (2017)	• Enables examination of the physiological response of a nonmodel organism • The importance of a biological pathway is evaluated by a specific inhibitor	• Applies to nonmodel organisms	• Some inhibitors are not specific to a single pathway • Action of inhibitors should be verified by a known physiological measurement

requires small amount of sample (10 mg), it is low cost, simple and quantitative. However, the detection is robust and cannot distinguish polymorphs and spatial distribution of chitin.

Chitin can be visualised microscopically by calcofluor white, which binds strongly to cellulose and chitin, and wheat-germ agglutinin (WGA), which binds to N-acetyl-D-glucosamine and sialic acid (Suzuki et al. 2007). Due to the nonspecific nature of calcofluor-white and WGA (Shillito et al. 1995), more specific detection is accomplished by using chitin-binding domain fused with green fluorescent protein (CBD-GFP), as shown in the larval shell of *Mytilus galloprovincialis* (Weiss & Schönitzer 2006) and the prismatic layer of *Atrina rigida* (Nudelman et al. 2007). Quantifying the expression of the chitin synthase gene is an alternative approach to measure chitin production (Cummings et al. 2011).

While the role of chitin may be essential in providing a waterproof cover and biomineralisation framework to the shell formation process, the plasticity of chitin synthesis under OA environmental stress has not yet been investigated. Chitin has many important biological roles in a diverse taxonomic group of animal models (Lee et al. 2011); therefore, the detection of chitin could provide valuable information on both the structural and functional responses to OA. The disadvantages of XRD, IR and pyrolysis NMR or GC-MS techniques for chitin analysis, such as the low abundance of organic materials in calcareous structures (and therefore time-consuming sample preparation), may limit the application of this approach to future OA studies. On the other hand, visualising chitin with dyes such as calcofluor white and WGA are prone to nonspecific reactivity to other molecules than chitin. The more specific CBD-GFP labeling requires a bioengineering protocol to express and purify the chitin probe.

Omics

Omics studies are generating 'big data'. However, these data cannot be simply used as proxies of fitness (Feder & Walser 2005). As a consequence, little information can be extracted from purely exploratory studies (e.g. comparisons between two OA scenarios). A more powerful approach involves the analysis of the data to test a hypothesis based on physiological or ecological experiments. For example, De Wit et al. (2016) filtered a large-scale transcriptomic database to select genes following the same pattern identified at the physiological level in copepods exposed to OA (Thor & Dupont 2015, De Wit et al. 2016). The future use of omics to investigate the effects of OA on biomineralisation is promising, especially using the integration of an omics technique with other physiological end points.

The three main omics approaches to consider are transcriptomics, proteomics and metabolomics. Transcriptomics is a study of messenger ribonucleic acid (mRNA) and actively expressed genes, while proteomics investigates the total protein profile and metabolomics capture the biochemical status of an organism.

Transcriptomic changes can provide insights into genetic pathways involved in calcification by comparison of gene expression (e.g. at different stages of calcification or under different environmental conditions). That is, when applied in a time series, changes in transcriptomes of developing larvae provide useful information relevant to the onset of biomineralisation (Zhang et al. 2012). De Wit et al. (2018) used OA as a tool to delay calcification in an early stage of oyster development and using a time series were able to identify genes involved in larval shell calcification (De Wit et al. 2018). Under OA, transcriptomic studies are used to assess the physiological capacity of organisms by studying not just the biomineralisation molecular pathways but also the other related pathways giving a complete picture in understanding the consequences of living in a high-CO_2 ocean (Todgham & Hofmann 2009).

Proteomics investigates the total protein profile. Because proteins are the active functional units of an expressed gene, these data are closer to the organism at the functional level and phenotype. Proteomes can be altered by OA, as shown by different calcification protein expressions in oysters (Dineshram et al. 2015). The organic matrix proteins that are associated with shell deposition have

been profiled in corals (Drake et al. 2013), oysters (Suzuki & Nagasawa 2013) and blue mussels (Suzuki et al. 2011), although this information has not been profiled in the OA context.

As with the transcriptome, some precautions should be taken during the interpretation of a proteome. The quantity of a protein commonly cannot be directly linked to the fitness of an organism as regulatory posttranslational modifications play a key role (Mann & Jensen 2003). This is an essential consideration for the study of shell proteins, which are often heavily glycosylated, phosphorylated or tyrosine-sulfated as required for calcium binding (Zhang & Zhang 2006).

A major disadvantage of applying omics to the study of biomineralisation is the low abundance of about 5% organic content in calcareous structures (Zhang & Zhang 2006). In order to isolate sufficient protein or polysaccharide for analysis, a large amount of shell must be used. In addition, the extraction and purification of the organic content is greatly influenced by decalcification, and the shell can often contain organic impurities (Watabe 1965). Researchers should be aware of technical limitations using different characterisation techniques; for example 2-dimensional gels have a lower sensitivity than isobaric tags for relative and absolute quantitation (iTRAQ) analysis (Wiese et al. 2007). In addition, the interpretation of omics data is highly dependent on genomic information; therefore, it remains as a challenging method for nonmodel organisms.

Cellular pH imaging

When live imaging is conducted, inverted microscopy enables living marine organisms to be fully submersed in seawater during observation (Venn et al. 2011, Stumpp et al. 2012, Tambutté et al. 2015, Chan et al. 2017). In some imaging methods, synthetic ratiometric images are generated by sequential images of the same region of interest. Mobile organisms can be immobilised (e.g. 2%–4% agarose seawater or using micropipettes) to enable image acquisition of the region of interest. For longer periods of observation, a perfusion chamber is necessary to remove metabolic waste and allow exchange of aerated experimental seawater with enriched CO_2.

Fluorescent microscopy has been applied to visualise the calcification compartment during mineralisation at a low seawater pH using markers including calcein, alizarin and calcofuor white for *in situ* analysis of calcification and tracking of calcification, as shown for coralline algae (Lewis & Diaz-Pulido 2017). Newly deposited minerals can be quantified from their fluorescent appearance at their respective excitation (Exλ) and emission wavelengths (Emλ) (e.g. alizarin: Exλ = 530–560 nm, Emλ = 580 nm; calcein: Exλ = 494 nm, Emλ = 517 nm; calcofluor white: Exλ = 365 nm, Emλ = 435 nm). Calcein is a preferable marker because of its high efficiency, noninvasiveness (Lewis & Diaz-Pulido 2017) and relatively low cost. In addition, the fluorescent region can be isolated and characterised using the techniques described for measuring growth and development in the earlier sections of this review.

The heterogenous distribution of carbon sources (e.g. CO_3^{2-} ions at the calcification site) can be monitored by measuring intracellular pH (de Nooijer et al. 2008, Venn et al. 2011, Venn et al. 2013, Tambutté et al. 2015). Similar to the carbonate dynamics in the ocean, a shift in pH influences the DIC abundance in the biomineralisation compartment, in terms of CO_3^{2-} and HCO_3^-. As shown in foraminifera, pH of the site of calcification increases during calcification, while the surrounding ambient pH decreases probably through active proton pumping (Toyofuku et al. 2017). A higher pH value facilitates the conversion of CO_2 and HCO_3^- to CO_3^{2-} (Toyofuku et al. 2017), and both the CO_3^{2-} concentration and $CaCO_3$ saturation state can then be calculated (Venn et al. 2011, 2013, Tambutté et al. 2015). Furthermore, it is possible to estimate the number of emitted protons by image processing of pH-sensitive ratiometric microsopy. Ratiometric fluorescent dyes enable the monitoring of intracellular and extracellular pH (Chan et al. 2015a, Comeau et al. 2017b, Toyofuku et al. 2017). Several pH-sensitive dyes are available depending on the tested pH range. When the cell-permeable dye SNARF-1 acetoxymethyl ester is excited at a wavelength of 543 nm, the ratio of fluorescence

captured at emission wavelengths of 585 ± 10 and 640 ± 10 nm shows a linear relationship to intracellular pH (Venn et al. 2013). Similarly, cell impermeable SNARF-1 can be used to measure pH in the calcifying fluid in corals; 2′-7′-bis(carboxyethyl)-5(6)-carboxyfluorescein (BCECF) for intracellular pH of echinoderm larvae (Stumpp et al. 2012) and pyranine for foraminifera (Toyofuku et al. 2017). This technique has been applied to OA to investigate how growth and calcification rates are affected by increasing pCO_2 (Stumpp et al. 2012), where extracellular pH was actively compensated.

More recently, measurement of intracellular pH employs the use of microelectrodes between 10- and 15-μm tip diameter for direct in-tissue measurement (Cai et al. 2016), using pH polymeric membrane microelectrodes (Zhao & Cai 1999) and CO_3^{2-} electrodes (Cai et al. 2016). Using this approach, pH and CO_3^{2-} were observed to sharply increase in the calcifying fluid of various coral species, confirming the presence of H^+ pump (Cai et al. 2016). In addition to intracellular pH determination, microelectrodes can be designed to monitor dissolved oxygen and calcium concentrations to enable analysis of a wider range of parameters (Glas et al. 2012a,b). The cellular pH-imaging techniques have an advantage of high spatial resolution for direct in-tissue measurement; however, the disadvantages include time-consuming sample preparation. This includes the challenge that organism immobilisation strategies vary and the protocol requires optimisation to ensure that the organism is capable of generating biominerals. Ratiometric pH probe also requires calibration before the ratios can be converted to pH values.

Physiological inhibitors and stimulators

The use of physiological inhibitors or stimulators is a useful approach to investigate the biochemical pathways and pumps involved with biomineralisation (Basse et al. 2015). How biological pathways may be influenced by specific inhibitors can explain the mechanism of shell formation under OA conditions. For example, treatment with adenylyl cyclase inhibitors alleviates the negative effects of OA in Pacific oysters, suggesting the potential mechanism change under OA (Wang et al. 2017). This result confirmed the role of adenosine triphosphate (ATP) generation is essential to support shell production (Pan et al. 2015). Not requiring complete genetic information is the greatest advantage of using inhibitors and stimulators to evaluate the mechanisms of biomineralisation in a reductionist approach (Toyofuku et al. 2017). However, the choice of inhibitors may be nonspecific to a single pathway, and its action requires verification by a known physiological end point.

Combining techniques

The techniques described in this review can be employed individually to answer specific scientific questions to determine the impact of OA on marine biomineralisation. However, it is important to consider combining techniques to address complex scientific questions.

Combining x-ray microscopy techniques

Due to the development of optimum sample preparation for the analysis of a flat surface (Perez-Huerta & Cusack 2009), the output of XPEEM with XAS (Fitzer et al. 2016) and SEM-EBSD (Hahn et al. 2012, Wolfe et al. 2013, Fitzer et al. 2014a,b) can be readily compared. This has allowed the influence of OA on both the biomineral structure and composition to be determined for corals (Rodolfo-Metalpa et al. 2011), sea urchins (Bray et al. 2014) and mussels (Melzner et al. 2011). Likewise, the simple mapping of calcite and aragonite is applicable across a wide variety of species, including mussels and limpets (Hahn et al. 2012, Langer et al. 2014, Fitzer et al. 2015a). In contrast, the comparison of mineral composition between high-resolution microscopy with spectral techniques such as XRD, FT-IR and XPEEM with XAS is more complex. The use of SEM imaging,

as well as calcite and aragonite thickness by EBSD or species-specific visual inspection using compound microscopy (Fitzer et al. 2014b), have their merits when it comes to examining larger areas of shell erosion. However, to examine the intricate details of biomineralisation and potential changes under OA conditions, these methods should be used in conjunction with XRD, FT-IR, XPEEM with XAS and SEM-EBSD.

Multiomics data integration

Several omics approaches can be integrated [i.e. multiomics (Huang et al. 2017)]. For example, the mantle transcriptome and shell proteomes were integrated to study the shell formation of the pearl oyster (Joubert et al. 2010, Berland et al. 2011), enabling proteomics data to be analysed without a complete genome. Similarly, proteomics and metabolomics were studied together in oysters (Wei et al. 2015). A more complex multiomics study examined the genome, transcriptome and proteome in the Pacific oyster (Zhang et al. 2012). Such a multiomics approach also provided insights into the phosphate biomineralisation in brachiopods (Luo et al. 2015). This is a promising approach in the context of OA to understand the fitness or survival of organisms.

Conclusions: What now for OA research on biomineralisation?

A range of tools to help researchers determine the impact of OA on biomineralisation mechanisms at physiological and molecular levels, and thus on shell or skeleton structural mechanics, have been discussed in this review, the purpose of which is to explore commonly available biomineralisation tools for understanding this single physiological response to OA. However, organisms have complex physiological profiles, and it is important to note that biomineralisation is not an isolated process, nor is it the only physiological process that needs to be considered in this context. Given the nature of biomineralisation mechanisms and their complex responses to OA, a variety of physiological, materials science and crystallography tools are needed to thoroughly understand the biomineralisation process and its vulnerability to OA.

This discussion outlines techniques that can be used to characterise, quantify and monitor the process of biomineralisation in a variety of calcifying marine organisms, especially when they are cultured under OA experimental conditions. It also highlights basic principles and the advantages and disadvantages of established, emerging and future techniques for OA researchers. The key to developing a strategy aimed at better understanding the potential consequences of OA is to define clear questions and hypotheses for testing. This would naturally lead to constraints (e.g. tested species, quantity of material available, size) that, when combined with practicalities (e.g. budget, equipment), will lead to selection of the appropriate experimental approach.

Recently, more attention has been paid to the underlying biological and physiological mechanisms of biomineralisation. For example, tissues and external organic layers can protect the shell from corrosion in undersaturated waters (Rodolfo-Metalpa et al. 2011). To address the underlying mechanisms affected by the impacts by OA, various methods need to be combined. For instance, determination of amorphous $CaCO_3$ is important to characterise mineral choice and relate phase transitions at the earliest stage of biomineral formation. Mechanisms of cellular involvement and specific biomolecules for biomineralisation can be examined using fluorescent microscopy and omics. The interactions of proteins in the extrapallial fluid and shell interface can be understood by applying techniques in isotope labelling and microscopy. It is also crucial to consider the fitness consequences of observed changes. For example, in a prey species, shell strength should be considered in relation to predator behaviour. The combination of established, emerging and future techniques will enable a holistic approach and better understanding of the potential impact of OA on biomineralisation by marine species and consequences for marine calcifiers and associated ecosystems.

Acknowledgements

The authors thank Andrew Mount, P. S. Murphy, Howard Browman and Kaimin Shih for their initial thoughts and input to this review at the 2nd Interdisciplinary Symposium on Ocean Acidification and Climate Change (ISOACC) meeting in Hong Kong in December 2016. We also appreciate Sylvie Tambutté and Alexander Venn for their comments and suggestions for this review. This research was supported by the University of Glasgow and University of Hong Kong Principal's Early Career Mobility Scheme awarded to SCF. SCF was supported by a NERC Independent Research Fellowship (NE/N01409X/1).

References

Addadi, L., Raz, S., and Weiner, S. 2003. Taking advantage of disorder: amorphous calcium carbonate and its roles in biomineralization. *Advanced Materials* **15**, 959–970.

Alfredsson, V. 2005. Cryo-TEM studies of DNA and DNA–lipid structures. *Current Opinion in Colloid & Interface Science* **10**, 269–273.

Allen, K.A., Hönisch, B., Eggins, S.M., and Rosenthal, Y. 2012. Environmental controls on B/Ca in calcite tests of the tropical planktic foraminifer species *Globigerinoides ruber* and *Globigerinoides sacculifer*. *Earth and Planetary Science Letters* **351–352**, 270–280.

Allison, N., Cohen, I., Finch, A.A., Erez, J., and Tudhope, A.W. 2014. Corals concentrate dissolved inorganic carbon to facilitate calcification. *Nature Communications* **5**, 5741.

Anstis, G., Chantikul, P., Lawn, B.R., and Marshall, D. 1981. A critical evaluation of indentation techniques for measuring fracture toughness: I, direct crack measurements. *Journal of the American Ceramic Society* **64**, 533–538.

Asnaghi, V., Chiantore, M., Mangialajo, L., Gazeau, F., Francour, P., Alliouane, S., and Gattuso, J.P. 2013. Cascading effects of ocean acidification in a rocky subtidal community. *PLOS ONE* **8**, e61978.

Basse, W.C., Gutowska, M.A., Findeisen, U., Stumpp, M., Dupont, S., Jackson, D.J., Himmerkus, N., Melzner, F., and Bleich, M. 2015. A sea urchin Na+K+2Cl− cotransporter is involved in the maintenance of calcification-relevant cytoplasmic cords in *Strongylocentrotus droebachiensis* larvae. *Comparative Biochemistry and Physiology Part A: Molecular & Integrative Physiology* **187**, 184–192.

Becker, J.S., Breuer, U., Hsieh, H.F., Osterholt, T., Kumtabtim, U., Wu, B., Matusch, A., Caruso, J.A., and Qin, Z. 2010. Bioimaging of metals and biomolecules in mouse heart by laser ablation inductively coupled plasma mass spectrometry and secondary ion mass spectrometry. *Analytical Chemistry* **82**, 9528–9533.

Beniash, E., Ivanina, A., Lieb, N.S., Kurochkin, I., and Sokolova, I.M. 2010. Elevated level of carbon dioxide affects metabolism and shell formation in oysters *Crassostrea virginica*. *Marine Ecology Progress Series* **419**, 95–108.

Berland, S., Marie, A., Duplat, D., Milet, C., Sire, J.Y., and Bédouet, L. 2011. Coupling proteomics and transcriptomics for the identification of novel and variant forms of mollusk shell proteins: a study with *P. margaritifera*. *Chembiochem* **12**, 950–961.

Bernhard, J.M., Blanks, J.K., Hintz, C.J., and Chandler, G.T. 2004. Use of the fluorescent calcite marker calcein to label foraminiferal tests. *Journal of Foraminiferal Research* **34**, 96–101.

Bradassi, F., Cumani, F., Bressan, G., and Dupont, S. 2013. Early reproductive stages in the crustose coralline alga Phymatolithon lenormandii are strongly affected by mild ocean acidification. *Marine Biology* **160**, 2261–2269.

Bray, L., Pancucci-Papadopoulou, M.A., and Hall-Spencer, J.M. 2014. Sea urchin response to rising pCO_2 shows ocean acidification may fundamentally alter the chemistry of marine skeletons. *Mediterranean Marine Science* **15**(3), 510–519. doi: http://dx.doi.org/10.12681/mms.579.

Butt, H.-J., Cappella, B., and Kappl, M. 2005. Force measurements with the atomic force microscope: technique, interpretation and applications. *Surface Science Reports* **59**, 1–152.

Butt, H.-J., Jaschke, M., and Ducker, W. 1995. Measuring surface forces in aqueous electrolyte solution with the atomic force microscope. *Bioelectrochemistry and Bioenergetics* **38**, 191–201.

Byrne, M., Lamare, M., Winter, D., Dworjanyn, S.A., and Uthicke, S. 2013. The stunting effect of a high CO_2 ocean on calcification and development in sea urchin larvae, a synthesis from the tropics to the poles. *Philosophical Transactions of the Royal Society of London. Series B, Biological Sciences* **368**, 20120439. doi: 10.1098.

Byrne, M., Smith, A.M., West, S., Collard, M., Dubois, P., Graba-landry, A., and Dworjanyn, S.A. 2014. Warming influences Mg^{2+} content, while warming and acidification influence calcification and test strength of a sea urchin. *Environmental Science & Technology* **48**, 12620–12627.

Cai, W.-J., Ma, Y., Hopkinson, B.M., Grottoli, A.G., Warner, M.E., Ding, Q., Hu, X., Yuan, X., Schoepf, V., Xu, H., Han, C., Melman, T.F., Hoadley, K.D., Pettay, D.T., Matsui, Y., Baumann, J.H., Levas, S., Ying, Y., and Wang, Y. 2016. Microelectrode characterization of coral daytime interior pH and carbonate chemistry. *Nature Communications* **7**, 11144. doi: 10.1038/ncomms11144.

Carricart-Ganivet, J.P., and Barnes, D.J. 2007. Densitometry from digitized images of X-radiographs: methodology for measurement of coral skeletal density. *Journal of Experimental Marine Biology and Ecology* **344**, 67–72.

Chan, V.B.S., Johnstone, M.B., Wheeler, M.P., and Mount, A.S. 2018. Chitin facilitated mineralization in the Eastern oyster. *Frontiers in Marine Science* **5**, Article 357.

Chan, V.B.S., Li., C., Lane, A.C., Wang, Y., Lu, X., Shih, K., Zhang, T., and Thiyagarajan, V. 2012. CO_2-driven ocean acidification alters and weakens integrity of the calcareous tubes produced by the serpulid tubeworm, *Hydroides elegans*. *PLOS ONE* **7**, e42718.

Chan, V.B.S., Toyofuku, T., Wetzel, G., Saraf, L., Thiyagarajan, V., and Mount, A.S. 2015a. Direct deposition of crystalline aragonite in the controlled biomineralization of the calcareous tubeworm. *Frontiers in Marine Science* **2**(97), 1–10. doi: 10.3389/fmars.2015.00097.

Chan, V.B.S., Vinn, O., Li, C., Lu, X., Kudryavtsev, A.B., Schopf, J.W., Shih, K., Zhang, T., and Thiyagarajan, V. 2015b. Evidence of compositional and ultrastructural shifts during the development of calcareous tubes in the biofouling tubeworm, *Hydroides elegans*. *Journal of Structural Biology* **189**, 230–237.

Chan, V.B.S., Toyofuku. T., Wetzel, G., Saraf, L., Thiyagarajan, V., and Mount, A.S. 2017. Characterization of calcification events using live optical and electron microscopy techniques in a marine tubeworm. *Journal of Visualized Experiments* **120**, e55164. doi:10.3791/55164.

Chatzinikolaou, E., Grigoriou, P., Keklikoglou, K., Faulwetter, S., and Papageorgiou, N. 2017. The combined effects of reduced pH and elevated temperature on the shell density of two gastropod species measured using micro-CT imaging. *ICES Journal of Marine Science: Journal du Conseil* **74**, 1135–1149.

Collard, M., Rastrick, S.P.S., Calosi, P., Demolder, Y., Dille, J., Findlay, H.S., Hall-Spencer, J.M., Milazzo, M., Moulin, L., Widdicombe, S., Dehairs, F., and Dubois, P. 2016. The impact of ocean acidification and warming on the skeletal mechanical properties of the sea urchin *Paracentrotus lividus* from laboratory and field observations. *ICES Journal of Marine Science* **73**, 727–738.

Comeau, S., Cornwall, C.E., and McCulloch, M.T. 2017a. Decoupling between the response of coral calcifying fluid pH and calcification to ocean acidification. *Scientific Reports* **7**, 7573. doi: 10.1038/s41598-017-08003-z.

Comeau, S., Tambutte, E., Carpenter, R.C., Edmunds, P.J., Evensen, N.R., Allemand, D., Ferrier-Pages, C., Tambutte, S., and Venn, A.A. 2017b. Coral calcifying fluid pH is modulated by seawater carbonate chemistry not solely seawater pH. *Proceedings of the Royal Society B-Biological Sciences* **284**, 20161669. doi: 10.1098/rspb.2016.1669.

Cooper, T.F., De'Ath, G., Fabricius, K.E., and Lough, J.M. 2008. Declining coral calcification in massive Porites in two nearshore regions of the northern Great Barrier Reef. *Global Change Biology* **14**, 529–538.

Cummings, V., Hewitt, J., Van Rooyen, A., Currie, K., Beard, S., Thrush, S., Norkko, J., Barr, N., Heath, P., Halliday, N.J., Sedcole, R., Gomez, A., McGraw, C., and Metcalf, V. 2011. Ocean acidification at high latitudes: potential effects on functioning of the Antarctic bivalve *Laternula elliptica*. *PLOS ONE* **6**:e16069.

Cyronak, T., Schulz, K.G., and Jokiel, P.L. 2016. The Omega myth: what really drives lower calcification rates in an acidifying ocean. *ICES Journal of Marine Science* **73**, 558–562.

Dalbeck, P., Cusack, M., Dobson, P.S., Allison, N., Fallick, A.E., and Tudhope, A.W. 2011. Identification and composition of secondary meniscus calcite in fossil coral and the effect on predicted sea surface temperature. *Chemical Geology* **280**, 314–322.

Davies, P.S. 1989. Short-term growth measurements of corals using an accurate buoyant weighing technique. *Marine Biology* **101**, 389–395.

de Nooijer, L.J., Toyofuku, T., Oguri, K., Nomaki, H., and Kitazato, H. 2008. Intracellular pH distribution in foraminifera determined by the fluorescent probe HPTS. *Limnology and Oceanography: Methods* **6**, 610–618.

deVries, M.S., Webb, S.J., Tu, J., Cory, E., Morgan, V., Sah, R.L., Deheyn, D.D., and Taylor, J.R.A. 2016. Stress physiology and weapon integrity of intertidal mantis shrimp under future ocean conditions. *Scientific Reports* **6**, 38637.

De Wit, P., Dupont, S., and Thor, P. 2016. Selection on oxidative phosphorylation and ribosomal structure as a multigenerational response to ocean acidification in the common copepod Pseudocalanus acuspes. *Evolutionary Applications* **9**, 1112–1123.

De Wit, P., Durland, E., Ventura, A., and Langdon, C.J. 2018. Gene expression correlated with delay in shell formation in larval Pacific oysters (*Crassostrea gigas*) exposed to experimental ocean acidification provides insights into shell formation mechanisms. *Bmc Genomics* **19**, 160.

Dickinson, G.H., Ivanina, A.V., Matoo, O.B., Portner, H.O., Lannig, G., Bock, C., Beniash, E., and Sokolova, I.M. 2012. Interactive effects of salinity and elevated CO_2 levels on juvenile eastern oysters, *Crassostrea virginica*. *The Journal of Experimental Biology* **215**, 29–43.

Dineshram, R., Sharma, R., Chandramouli, K., Yalamanchili, H.K., Chu, I., and Thiyagarajan, V. 2015. Comparative and quantitative proteomics reveal the adaptive strategies of oyster larvae to ocean acidification. *Proteomics* **15**, 4120–4134.

Doney, S.C., Fabry, V.J., Feely, R.A., and Kleypas, J.A. 2009. Ocean acidification: the other CO_2 problem. *Annual Review of Marine Science* **1**, 169–192.

Drake, J.L., Mass, T., Haramaty, L., Zelzion, E., Bhattacharya, D., and Falkowski, P.G. 2013. Proteomic analysis of skeletal organic matrix from the stony coral *Stylophora pistillata*. *Proceedings of the National Academy of Sciences* **110**, 3788–3793.

Dwyer, G.S., Cronin, T.M. and Baker, P.A. 2013. Trace elements in marine ostracodes. In J.A. Holmes & A.R. Chivas (eds), *The Ostracoda: applications in Quaternary Research. Geophys. Monogr. Series.*, AGU, Washington, 205–225.

Eichner, M.J., Klawonn, I., Wilson, S.T., Littmann, Whitehouse, S.M.J., Church, M.J., Kuypers, M.M.M., Karl, D.M., and Ploug, H. 2017. Chemical microenvironments and single-cell carbon and nitrogen uptake in field-collected colonies of Trichodesmium under different pCO_2. *Isme Journal* **11**, 1305.

Eisenstein, N.M., Cox, S.C., Williams, R.L., Stapley, S.A., and Grover, L.M. 2016. Bedside, benchtop, and bioengineering: physicochemical imaging techniques in biomineralization. *Advanced Healthcare Materials* **5**, 507–528.

Elderfield, H., Bertram, C.J., and Erez, J. 1996. A biomineralization model for the incorporation of trace elements into foraminiferal calcium carbonate. *Earth and Planetary Science Letters* **142**, 409–423.

Erez, J. 1978. Vital effect on stable-isotope composition seen in foraminifera and coral skeletons. *Nature* **273**, 199.

Falini, G., Weiner, S., and Addadi, L. 2003. Chitin-silk fibroin interactions: relevance to calcium carbonate formation in invertebrates. *Calcified Tissue International* **72**, 548–554.

Fang, J.K., Schoenberg, C.H., Kline, D.I., Hoegh-Guldberg, O., and Dove, S. 2013. Methods to quantify components of the excavating sponge *Cliona orientalis* Thiele, 1900. *Marine Ecology* **34**, 193–206.

Fantazzini, P., Mengoli, S., Pasquini, L., Bortolotti, V., Brizi, L., Mariani, M., Di Giosia, M., Fermani, S., Capaccioni, B., Caroselli, E., Prada, F., Zaccanti, F., Levy, O., Dubinsky, Z., Kaandorp, J.A., Konglerd, P., Hammel, J.U., Dauphin, Y., Cuif, J.-P., Weaver, J.C., Fabricius, K.E., Wagermaier, W., Fratzl, P., Falini, G., and Goffredo, S. 2015. Gains and losses of coral skeletal porosity changes with ocean acidification acclimation. *Nature Communications* **6**, 7785. doi: 10.1038/ncomms8785.

Feder, M.E., and Walser, J.C. 2005. The biological limitations of transcriptomics in elucidating stress and stress responses. *Journal of Evolutionary Biology* **18**, 901–910.

Feely, R.A., Sabine, C.L., Lee, K., Berelson, W., Kleypas, J., Fabry, V.J., and Millero, F.J. 2004. Impact of anthropogenic CO_2 on the $CaCO_3$ system in the oceans. *Science* **305**(5682), 362–366. doi: 10.1126/science.1097329

Fietzke, J., Heinemann, A., Taubner, I., Böhm, F., Erez, J., and Eisenhauer, A. 2010. Boron isotope ratio determination in carbonates via LA-MC-ICP-MS using soda-lime glass standards as reference material. *Journal of Analytical Atomic Spectrometry* **25**, 1953–1957.

Fitzer, S. Chung, C.P., Maccherozzi, F., Dhesi, S.S., Kamenos, N.A., Phoenix, V.R., and Cusack, M. 2016. Biomineral shell formation under ocean acidification: a shift from order to chaos. *Scientific Reports* **6**, 21076. doi: 10.1038/srep21076.

Fitzer, S.C., Cusack, M., Phoenix, V.R., and Kamenos, N.A. 2014a. Ocean acidification reduces the crystallographic control in juvenile mussel shells. *Journal of Structural Biology* **188**, 39–45.

Fitzer, S.C., Phoenix, V.R., Cusack, M., and Kamenos, N.A. 2014b. Ocean acidification impacts mussel control on biomineralisation. *Scientific Reports* **4**, 6218. doi: 10.1038/srep06218.

Fitzer, S.C., Vittert, L., Bowman, A., Kamenos, N.A., Phoenix, V.R., and Cusack, M. 2015a. Ocean acidification and temperature increase impact mussel shell shape and thickness: problematic for protection? *Ecology and Evolution* **5**, 4875–4884.

Fitzer, S.C., Zhu, W., Tanner, K.E., Kamenos, N.A., Phoenix, V.R., and Cusack, M. 2015b. Ocean acidification alters the material properties of *Mytilus edulis* shells. *Journal of the Royal Society Interface* **12**, 20141227.

Freeman, A.S., and Byers J.E. 2006. Divergent induced responses to an invasive predator in marine mussel populations. *Science* **313**, 831–833. doi: 10.1126/science.1125485

Frieder, C.A., Applebaum, S.L., Pan, T.C.F., Hedgecock, D., and Manahan, D.T. 2016. Metabolic cost of calcification in bivalve larvae under experimental ocean acidification. *ICES Journal of Marine Science* **74**(4), 941–954. doi: https://doi.org/10.1093/icesjms/fsw213

Fu, J.M., He, C., Xia, B., Li, Y., Feng, Q., Yin, Q.F., Shi, X.H., Feng, X., Wang, H.T., and Yao, H.M. 2016. c-axis preferential orientation of hydroxyapatite accounts for the high wear resistance of the teeth of black carp (*Mylopharyngodon piceus*). *Scientific Reports* **6**, 23509. doi: 10.1038/srep23509.

Furla, P., Galgani, I., Durand, I., and Allemand, D. 2000. Sources and mechanisms of inorganic carbon transport for coral calcification and photosynthesis. *Journal of Experimental Biology* **203**, 3445–3457.

Furuhashi, T., Beran, A., Blazso, M., Czegeny, Z., Schwarzinger, C., and Steiner, G. 2009. Pyrolysis GC/MS and IR spectroscopy in chitin analysis of molluscan shells. *Bioscience, Biotechnology, and Biochemistry* **73**, 93–103.

Gao, K., Ruan, Z., Villafañe, V.E., Gattuso, J.-P., and Helbling, E.W. 2009. Ocean acidification exacerbates the effect of UV radiation on the calcifying phytoplankter *Emiliania huxleyi*. *Limnology and Oceanography* **54**, 1855–1862.

Gazeau, F., Quiblier, C., Jansen, J.M., Gattuso, J.-P., Middelburg, J.J., and Heip, C.H.R. 2007. Impact of elevated CO_2 on shellfish calcification. *Geophysical Research Letters* **34**(7), L07603.

Ghosh, P., Adkins, J., Affek, H., Balta, B., Guo, W., Schauble, E.A., Schrag, D., and Eiler, J.M. 2006. 13C–18O bonds in carbonate minerals: a new kind of paleothermometer. *Geochimica et Cosmochimica Acta* **70**, 1439–1456.

Glas, M.S., Fabricius, K.E., de Beer, D., and Uthicke, S. 2012a. The O_2, pH and Ca^{2+} microenvironment of benthic foraminifera in a high CO_2 world. *PLOS ONE* **7**, e50010. doi: 10.1371/journal.pone.0050010.

Glas, M.S., Langer, G., and Keul, N. 2012b. Calcification acidifies the microenvironment of a benthic foraminifer (Ammonia sp.). *Journal of Experimental Marine Biology and Ecology* **424–425**, 53–58.

Goffredo, S., Prada, F., Caroselli, E., Capaccioni, B., Zaccanti, F., Pasquini, L., Fantazzini, P., Fermani, S., Reggi, M., Levy, O., Fabricius, K.E., Dubinsky, Z., and Falini, G. 2014. Biomineralization control related to population density under ocean acidification. *Nature Climate Change* **4**, 593–597.

Gong, Y.U.T., Killian, C.E., Olson, I.C., Appathurai, N.P., Amasino, A.L., Martin, M.C., Holt, L.J., Wilt, F.H., and Gilbert, P.U.P.A. 2012. Phase transitions in biogenic amorphous calcium carbonate. *PNAS* **109**, 6088–6093.

Guidetti, P., and Mori, M. 2005. Morpho-functional defences of Mediterranean sea urchins, *Paracentrotus lividus* and *Arbacia lixula*, against fish predators. *Marine Biology* **147**, 797–802.

Guo, W., Mosenfelder, J.L., Goddard III, W.A., and Eiler, J.M. 2009. Isotopic fractionations associated with phosphoric acid digestion of carbonate minerals: insights from first-principles theoretical modeling and clumped isotope measurements. *Geochimica et Cosmochimica Acta* **73**, 7203–7225.

Hahn, S., Rodolfo-Metalpa, R., Griesshaber, E., Schmahl, W.W., Buhl, D., Hall-Spencer, J.M., Baggini, C., Fehr, K.T., and Immenhauser, A. 2012. Marine bivalve shell geochemistry and ultrastructure from modern low pH environments: environmental effect versus experimental bias. *Biogeosciences* **9**, 1897–1914.

Harney, E., Artigaud, S., Le Souchu, P., Miner, P., Corporeau, C., Essid, H., Pichereau, V., and Nunes, F.L.D. 2016. Non-additive effects of ocean acidification in combination with warming on the larval proteome of the Pacific oyster, *Crassostrea gigas*. *Journal of Proteomics* **135**, 151–161.

Hemming, N.G., and Hanson, G.N. 1992. Boron isotopic composition and concentration in modern marine carbonates. *Geochimica et Cosmochimica Acta* **56**, 537–543.

Hennige, S.J., Wicks, L.C., Kamenos, N.A., Perna, G., Findlay, H.S., Roberts, J.M. 2015. Hidden impacts of ocean acidification on live and dead coral framework. *Proceedings of the Royal Society B*. **282**, 20150990. http://dx.doi.org/10.1098/rspb.2015.0990

Herler, J., and Dirnwöber, M. 2011. A simple technique for measuring buoyant weight increment of entire, transplanted coral colonies in the field. *Journal of Experimental Marine Biology and Ecology* **407**, 250–255.

Hofmann, G.E., O'Donnell, M.J., and Todgham, A.E. 2008. Using functional genomics to explore the effects of ocean acidification on calcifying marine organisms. *Marine Ecology Progress Series* **373**, 219–226.

Huang, S., Chaudhary, K., and Garmire, L.X. 2017. More is better: recent progress in multi-omics data integration methods. *Frontiers in Genetics* **8**(84), 1–12. https://doi.org/10.3389/fgene.2017.00084.

Iglesias-Rodriguez, M.D., Halloran, P.R., Rickaby, R.E.M., Hall, I.R., Colmenero-Hidalgo, E., Gittins, J.R., Green, D.R.H., Tyrrell, T., Gibbs, S.J., von Dassow, P., Rehm, E., Armbrust, E.V., and Boessenkool, K.P. 2008. Phytoplankton calcification in a high-CO_2 world. *Science* **320**, 336–340.

Jeffree, R.A., Markich, S.J., Lefebvre, F., Thellier, M., and Ripoll, C. 1995. Shell microlaminations of the freshwater bivalveHyridella depressa as an archival monitor of manganese water concentration: experimental investigation by depth profiling using secondary ion mass spectrometry (SIMS). *Experientia* **51**, 838–848.

Jokiel, P.L., Rodgers, K.S., Kuffner, I.B., Andersson, A.J., Cox, E.F., and Mackenzie, F.T. 2008. Ocean acidification and calcifying reef organisms: a mesocosm investigation. *Coral Reefs* **27**, 473–483.

Joubert, C., Piquemal, D., Marie, B., Manchon, L., Pierrat, F., Zanella-Cléon, I., Cochennec-Laureau, N., Gueguen, Y., and Montagnani, C. 2010. Transcriptome and proteome analysis of Pinctada margaritifera calcifying mantle and shell: focus on biomineralization. *Bmc Genomics* **11**, 613.

Kamenos, N.A., Burdett, H.L., Aloisio, E., Findlay, H.S., Martin, S., Longobone, C., Dunn, J. Widdicombe, S., and Calosi, P. 2013. Coralline algal structure is more sensitive to rate, rather than the magnitude, of ocean acidification. *Global Change Biology* **19**, 3621–3628.

Katano, H., Takakuwa, M., Hayakawa, H., and Kimoto, H. 2016. Determination of chitin based on the colorimetric assay of glucosamine in acid hydrolysate. *Analytical Sciences* **32**, 701–703.

Keul, N., Langer, G., de Nooijer, L.J., Nehrke, G., Reichart, G.J., and Bijma, J. 2013. Incorporation of uranium in benthic foraminiferal calcite reflects seawater carbonate ion concentration. *Geochemistry, Geophysics, Geosystems* **14**, 102–111.

Khalifa, G.M., Kirchenbuechler, D., Koifman, N., Kleinerman, O., Talmon, Y., Elbaum, M., Addadi, L., Weiner, S., and Erez, J. 2016. Biomineralization pathways in a foraminifer revealed using a novel correlative cryo-fluorescence–SEM–EDS technique. *Journal of Structural Biology* **196**, 155–163.

Kikuchi, S. 1928. Diffraction of cathode rays by mica. *Proceedings of the Imperial Academy* **4**, 354–356.

Krief, S., Hendy, E.J., Fine, M., Yam, R., Meibom, A., Foster, G.L., and Shemesh, A. 2010. Physiological and isotopic responses of scleractinian corals to ocean acidification. *Geochimica et Cosmochimica Acta* **74**, 4988–5001.

Kruzic, J.J., Kim, D.K., Koester, K.J., and Ritchie, R.O. 2009. Indentation techniques for evaluating the fracture toughness of biomaterials and hard tissues. *Journal of the Mechanical Behavior of Biomedical Materials* **2**, 384–395.

Kunitake, M.E., Baker, S.P., and Estroff, L.A. 2012. The effect of magnesium substitution on the hardness of synthetic and biogenic calcite. *MRS Communications* **2**, 113–116.

Kunitake, M.E., Mangano, L.M., Peloquin, J.M., Baker, S.P., and Estroff, L.A. 2013. Evaluation of strengthening mechanisms in calcite single crystals from mollusk shells. *Acta Biomaterialia* **9**, 5353–5359.

Langdon, C., and Atkinson, M.J. 2005. Effect of elevated pCO_2 on photosynthesis and calcification of corals and interactions with seasonal change in temperature/irradiance and nutrient enrichment. *Journal of Geophysical Research: Oceans* **110**, C09S07.

Langdon, C., Takahashi, T., Sweeney, C., Chipman, D., Goddard, J., Marubini, F., Aceves, H., Barnett, H., and Atkinson, M.J. 2000. Effect of calcium carbonate saturation state on the calcification rate of an experimental coral reef. *Global Biogeochemical Cycles* **14**, 639–654.

Langer, G., Nehrke, G., Baggini, C., Rodolfo-Metalpa, R., Hall-Spencer, J.M., and Bijma, J. 2014. Limpets counteract ocean acidification induced shell corrosion by thickening of aragonitic shell layers. *Biogeosciences* **11**, 7363–7368.

Lawn, B.R., Evans, A., and Marshall, D. 1980. Elastic/plastic indentation damage in ceramics: the median/radial crack system. *Journal of the American Ceramic Society* **63**, 574–581.

Lear, C.H., Elderfield, H., and Wilson, P.A. 2000. Cenozoic deep-sea temperatures and global ice volumes from Mg/Ca in benthic foraminiferal calcite. *Science* **287**, 269–272.

Lee, C.G., Da Silva, C.A., Dela Cruz, C.S., Ahangari, F., Ma, B., Kang, M.J., He, C.H., Takyar, S., and Elias, J.A. 2011. Role of chitin and chitinase/chitinase-like proteins in inflammation, tissue remodeling, and injury. *Annual Review of Physiology* **73**, 479–501.

Leung, J.Y., Russell, B.D., and Connell, S.D. 2017. Mineralogical plasticity acts as a compensatory mechanism to the impacts of ocean acidification. *Environmental Science & Technology* **51**(5), 2652–2659.

Levi-Kalisman, Y., Falini, G., Addadi, L., and Weiner, S. 2001. Structure of the nacreous organic matrix of a bivalve mollusk shell examined in the hydrated state using cryo-TEM. *Journal of Structural Biology* **135**, 8–17.

Lewis, B., and Diaz-Pulido, G. 2017. Suitability of three fluorochrome markers for obtaining in situ growth rates of coralline algae. *Journal of Experimental Marine Biology and Ecology* **490**, 64–73.

Li, C., Chan, V.B.S., He, C., Meng, Y., Yao, H., Shih, K., and Thiyagarajan, V. 2014. Weakening mechanisms of the serpulid tube in a high-CO_2 world. *Environmental Science & Technology* **48**, 14158–14167.

Li, C., Meng, Y., He, C., Chan, V.B.S., Yao, H., and Thiyagarajan, V. 2016. Mechanical robustness of the calcareous tubeworm *Hydroides elegans*: warming mitigates the adverse effects of ocean acidification. *Biofouling* **32**, 191–204.

Li, Y., Zhuang, S., Wu, Y., Ren, H., Cheng, F., Lin, X., Wang, K., Beardall, J., and Gao, K. 2015. Ocean acidification modulates expression of genes and physiological performance of a marine diatom. *Biogeosciences Discuss* **2015**, 15809–15833.

Limbeck, A., Bonta, M., and Nischkauer, W. 2017. Improvements in the direct analysis of advanced materials using ICP-based measurement techniques. *Journal of Analytical Atomic Spectrometry* **32**, 212–232.

Lombardi, C., Cocito, S., Gambi, M.C., and Taylor, P.D. 2015. Morphological plasticity in a calcifying modular organism: evidence from an *in situ* transplant experiment in a natural CO_2 vent system. *Royal Society Open Science* **2**(2), 140413. doi: 10.1098/rsos.140413.

Luo, Y.-J., Takeuchi, T., Koyanagi, R., Yamada, L., Kanda, M., Khalturina, M., Fujie, M., Yamasaki, S.-I., Endo, K., and Satoh, N. 2015. The *Lingula* genome provides insights into brachiopod evolution and the origin of phosphate biomineralization. *Nature Communications* **6**, 8301. doi: 10.1038/ncomms9301.

Mackenzie, C.L., Ormondroyd, G.A., Curling, S.F., Ball, R.J., Whiteley, N.M., and Malham, S.K. 2014. Ocean warming, more than acidification, reduces shell strength in a commercial shellfish species during food limitation. *PLOS ONE* **9**, e86764. doi:10.1371/journal.pone.0086764.

Mann, M., and Jensen, O.N. 2003. Proteomic analysis of post-translational modifications. *Nature Biotechnology* **21**, 255–261.

Marie, B., Le Roy, N., Zanella-Cléon, I., Becchi, M., and Marin, F. 2011. Molecular evolution of mollusc shell proteins: insights from proteomic analysis of the edible mussel *Mytilus*. *Journal of Molecular Evolution* **72**, 531–546.

Marie, B., Marie, A., Jackson, D.J., Dubost, L., Degnan, B.M., Milet, C., and Marin, F. 2010. Proteomic analysis of the organic matrix of the abalone *Haliotis asinina* calcified shell. *Proteome Science* **8**, 54. doi: 10.1186/1477-5956-8-54.

Marsh, J.A. 1970. Primary productivity of reef-building calcareous red algae. *Ecology* **51**, 255–263.

Martin, P.A., and Lea, D.W. 2002. A simple evaluation of cleaning procedures on fossil benthic foraminiferal Mg/Ca. *Geochemistry, Geophysics, Geosystems* **3**, 1–8.

Martin, P., Goodkin, N.F., Stewart, J.A., Foster, G.L., Sikes, E.L., White, H.K., Hennige, S., and Roberts, J.M. 2016. Deep-sea coral δ13C: a tool to reconstruct the difference between seawater pH and δ11B-derived calcifying fluid pH. *Geophysical Research Letters* **43**, 299–308.

Marxen, J.C., Nimtz, M., Becker, W., and Mann, K. 2003. The major soluble 19.6 kDa protein of the organic shell matrix of the freshwater snail *Biomphalaria glabrata* is an N-glycosylated dermatopontin. *Biochimica et Biophysica Acta (BBA)-Proteins and Proteomics* **1650**, 92–98.

McConnaughey, T.A., and Gillikin, D.P. 2008. Carbon isotopes in mollusk shell carbonates. *Geo-Marine Letters* **28**, 287–299.

McEnery, M., and Lee, J.J. 1970. Tracer studies on calcium and strontium mineralization and mineral cycling in two species of foraminifera, *Rosalina leei* and *Spiroloculina hyalina*. *Limnology and Oceanography* **15**, 173–182.

Melbourne, L.A., Griffin, J., Schmidt, D.N., and Rayfield, E.J. 2015. Potential and limitations of finite element modelling in assessing structural integrity of coralline algae under future global change. *Biogeosciences* **12**(15), 5891–5883. doi: 10.5194/bg-12-5871-2015.

Melzner, F., Stange, P., Trubenbach, K., Thomsen, J., Casties, I., Panknin, U., Gorb, S.N., and Gutowska, M.A. 2011. Food supply and seawater pCO_2 impact calcification and internal shell dissolution in the blue mussel *Mytilus edulis*. *PLOS ONE* **6**, e24223. doi: 10.1371/journal.pone.0024223.

Milano, S., Schöne, B.R., Wang, S., and Müller, W.E. 2016. Impact of high pCO_2 on shell structure of the bivalve *Cerastoderma edule*. *Marine Environmental Research* **119**, 144–155.

Milazzo, M., Rodolfo-Metalpa, R., Chan, V.B.S., Fine, M., Alessi, C., Thiyagarajan, V., Hall-Spencer, J.M., and Chemello, R. 2014. Ocean acidification impairs vermetid reef recruitment. *Scientific Reports* **4**, 4189.

Miyamoto, H., Miyashita, T., Okushima, M., Nakano, S., Morita, T., and Matsushiro, A. 1996. A carbonic anhydrase from the nacreous layer in oyster pearls. *Proceedings of the National Academy of Sciences* **93**, 9657–9660.

Molina, R., Hanlon, S., Savidge, T., Bogan, A., and Levine, J. 2005. Buoyant weight technique: application to freshwater bivalves. *American Malacological Bulletin* **20**, 49–53.

Müller, M.N., Kısakürek, B., Buhl, D., Gutperlet, R., Kolevica, A., Riebesell, U., Stoll, H., and Eisenhauer, A. 2011. Response of the coccolithophores *Emiliania huxleyi* and *Coccolithus braarudii* to changing seawater Mg^{2+} and Ca^{2+} concentrations: Mg/Ca, Sr/Ca ratios and δ44/40Ca, δ26/24Mg of coccolith calcite. *Geochimica et Cosmochimica Acta* **75**, 2088–2102.

Naddafi, R., and Rudstam, L.G. 2014. Predator induced morphological change in dreissenid mussels: implications for species replacement. *Freshwater Biology* **59**, 703–713.

Nakayama, S., Suzuki, M., Endo, H., Limura, K., Kinoshita, S., Watabe, S., Kogure, T., and Nagasawa, H. 2013. Identification and characterization of a matrix protein (PPP-10) in the periostracum of the pearl oyster, *Pinctada fucata*. *FEBS Open Bio* **3**, 421–427.

Nellist, P.D., Chisholm, M.F., Dellby, N., Krivanek, O.L., Murfitt, M.F., Szilagyi, Z.S., Lupini, A.R., Borisevich, A., Sides, W.H., and Pennycook, S.J. 2004. Direct sub-angstrom imaging of a crystal lattice. *Science* **305**, 1741–1741.

Newbury, D.E. 1998. Trace element detection at nanometer scale spatial resolution. *Microscopy* **47**, 407–418.

Nimer, N.A., and Merrett, M.J. 1993. Calcification rate in *Emiliania huxleyi* Lohmann in response to light, nitrate and availability of inorganic carbon. *New Phytologist* **123**, 673–677.

Nishikawa, S., and Kikuchi, S. 1928. Diffraction of cathode rays by calcite. *Nature* **122**, 726–726.

Norzagaray-López, O.C., Calderon-Aguilera, L.E., Castro-Ceseña, A.B., Hirata, G., and Hernández-Ayón, J.M. 2017. Skeletal dissolution kinetics and mechanical tests in response to morphology among coral genera. *Facies* **63**, 7. doi: 10.1007/s10347-016-0488-2.

Not, C., Thibodeau, B., and Yokoyama, Y. 2018. Incorporation of Mg, Sr, Ba, U, and B in high-Mg calcite benthic foraminifers cultured under controlled pCO_2. *Geochemistry, Geophysics, Geosystems* **19**, 83–98.

Nudelman, F., Chen, H.H., Goldberg, H.A., Weiner, S., Addadi, L. 2007. Spiers Memorial Lecture. Lessons from biomineralization: comparing the growth strategies of mollusc shell prismatic and nacreous layers in *Atrina rigida*. *Faraday Discussions* **136**, 9–25.

Nürnberg, D., Bijma, J., and Hemleben, C. 1996. Assessing the reliability of magnesium in foraminiferal calcite as a proxy for water mass temperatures. *Geochimica et Cosmochimica Acta* **60**, 803–814.

Oliver, W.C., and Pharr, G.M. 1992. An improved technique for determining hardness and elastic modulus using load and displacement sensing indentation experiments. *Journal of Materials Research* **7**, 1564–1583.

Orr, J.C., Fabry, V.J., Aumont, O., Bopp, L., Doney, S.C., Feely, R.A., Gnanadesikan, A., Gruber, N., Ishida, A., and Joos, F. 2005. Anthropogenic ocean acidification over the twenty-first century and its impact on calcifying organisms. *Nature* **437**, 681–686.

Paasche, E. 1963. The adaptation of the carbon-14 method for the measurement of coccolith production in *Coccolithus huxleyi*. *Physiologia Plantarum* **16**, 186–200.

Pan, T.C.F., Applebaum, S.L., and Manahan, D.T. 2015. Experimental ocean acidification alters the allocation of metabolic energy. *Proceedings of the National Academy of Sciences* **112**, 4696–4701.

Parkinson, D., Curry, G.B., Cusack, M., and Fallick, A.E. 2005. Shell structure, patterns and trends of oxygen and carbon stable isotopes in modern brachiopod shells. *Chemical Geology* **219**, 193–235.

Pearson, F., Marchessault, R., and Liang, C. 1960. Infrared spectra of crystalline polysaccharides. V. Chitin. *Journal of Polymer Science* **43**, 101–116.

Perez-Huerta, A., and Cusack, M. 2009. Optimizing electron backscatter diffraction of carbonate biominerals-resin type and carbon coating. *Microscopy and Microanalysis* **15**, 197–203.

Pérez-Huerta, A., Cusack, M., Jeffries, T.E., and Williams, C.T. 2008. High resolution distribution of magnesium and strontium and the evaluation of Mg/Ca thermometry in Recent brachiopod shells. *Chemical Geology* **247**, 229–241.

Politi, Y., Levi-Kalisman, Y., Raz, S., Wilt, F., Addadi, L., Weiner, S., and Sagi, I. 2006. Structural characterization of the transient amorphous calcium carbonate precursor phase in sea urchin embryos. *Advanced Functional Materials* **16**, 1289–1298.

Politi, Y., Metzler, R.A., Abrecht, M., Gilbert, B., Wilt, F.H., Sagi, I., Addadi, L., Weiner, S., and Gilbert, P.U.P.A. 2008. Transformation mechanism of amorphous calcium carbonate into calcite in the sea urchin larval spicule. *Proceedings of the National Academy of Sciences of the United States of America* **105**, 17362–17366.

Rae, J.W.B., Foster, G.L., Schmidt, D.N., and Elliott, T. 2011. Boron isotopes and B/Ca in benthic foraminifera: proxies for the deep ocean carbonate system. *Earth and Planetary Science Letters* **302**, 403–413.

Ragazzola, F., Foster, L.C., Form, A., Anderson, P.S.L., Hansteen, T.H., and Fietzke, J. 2012. *Global Change Biology* **18**(9), 2804–2812. doi: 10.1111/j.1365-2486.2012.02756.x.

Raven, J., Caldeira, K., Elderfield, H., Hoegh-Guldberg, O., Liss, P.S., Riebesell, U., Sheperd, J., Turley, C., and Watson, A. 2005. *Ocean Acidification Due to Increasing Atmospheric Carbon Dioxide*. London: The Royal Society, 1–68.

Reynaud, S., Leclercq, N., Romaine-Lioud, S., Ferrier-Pages, C., Jaubert, J., and Gattuso, J. P. 2003. Interacting effects of CO_2 partial pressure and temperature on photosynthesis and calcification in a scleractinian coral. *Global Change Biology* **9**, 1660–1668.

Riebesell, U., Zondervan, I., Rost, B., Tortell, P.D., Zeebe, R.E., and Morel, F.M.M. 2000. Reduced calcification of marine plankton in response to increased atmospheric CO_2. *Nature* **407**, 364–367.

Ries, J.B., Cohen, A.L., and McCorkle, D.C. 2009. Marine calcifiers exhibit mixed responses to CO_2-induced ocean acidification. *Geology* **37**, 1131–1134.

Rodolfo-Metalpa, R., Houlbreque, F., Tambutte, E., Boisson, F., Baggini, C., Patti, F.P., Jeffree, R., Fine, M., Foggo, A., Gattuso, J.P., and Hall-Spencer, J.M. 2011. Coral and mollusc resistance to ocean acidification adversely affected by warming. *Nature Climate Change* **1**, 308–312.

Rodolfo-Metalpa, R., Montagna, P., Aliani, S., Borghini, M., Canese, S., Hall-Spencer, J.M., Foggo, A., Milazzo, M., Taviani, M., and Houlbrèque, F. 2015. Calcification is not the Achilles' heel of cold-water corals in an acidifying ocean. *Global Change Biology* **21**, 2238–2248.

Roleda, M.Y., Boyd, P.W., and Hurd, C.L. 2012. Before ocean acidification: calcifier chemistry lessons. *Journal of Phycology* **48**, 840–843.

Rühl, S., Calosi, P., Faulwetter, S., Keklikoglou, K., Widdicombe, S., and Queirós, A.M. 2017. Long-term exposure to elevated pCO_2 more than warming modifies early-life shell growth in a temperate gastropod. *ICES Journal of Marine Science* **74**, 1113–1124.

Sabatier, P., Reyss, J.L., Hall-Spencer, J.M., Colin, C., Frank, N., Tisnérat-Laborde, N., Bordier, L., and Douville, E. 2012. ^{210}Pb-^{226}Ra chronology reveals rapid growth rate of *Madrepora oculata* and *Lophelia pertusa* on world's largest cold-water coral reef. *Biogeosciences* **9**, 1253–1265.

Samata, T., Hayashi, N., Kono, M., Hasegawa, K., Horita, C., and Akera, S. 1999. A new matrix protein family related to the nacreous layer formation of *Pinctada fucata*. *FEBS Letters* **462**, 225–229.

Satoh, M., Iwamoto, K., Suzuki, I., and Shiraiwa, Y. 2009. Cold stress stimulates intracellular calcification by the coccolithophore, *Emiliania huxleyi* (Haptophyceae) under phosphate-deficient conditions. *Marine Biotechnology* **11**, 327–333.

Schoepf, V., Hu, X., Holcomb, M., Cai, W.J., Li, Q., Wang, Y., Xu, H., Warner, M.E., Melman, T.F., Hoadley, K.D., Pettay, D.T., Matsui, Y., Baumann, J.H., and Grottoli, A.G. 2017. Coral calcification under environmental change: a direct comparison of the alkalinity anomaly and buoyant weight techniques. *Coral Reefs* **36**, 13–25.

Shillito, B., Lubbering, B., Lechaire, J-P., Childress, J.J., and Gail, F. 1995. Chitin localization in the tube secretion system of a repressurized deep-sea tube worm. *Journal of Structural Biology* **114**, 67–75.

Sikes, C.S., Wheeler, A.P., Wierzbicki, A., Mount, A.S., and Dillaman, R.M. 2000. Nucleation and growth of calcite on native versus pyrolyzed oyster shell folia. *Biological Bulletin* **198**, 50–66.

Sinclair, D.J. 2005. Correlated trace element 'vital effects' in tropical corals: a new geochemical tool for probing biomineralization. *Geochimica et Cosmochimica Acta* **69**, 3265–3284.

Singh, S.K., and Sigworth, F.J. 2015. Cryo-EM: spinning the micelles away. *Structure* **23**, 1561. doi: 10.1016/j.str.2015.08.001.

Spero, H.J., Bijma, J., Lea, D.W., and Bemis, B.E. 1997. Effect of seawater carbonate concentration on foraminiferal carbon and oxygen isotopes. *Nature* **390**, 497–500.

Stewart, J.A., Anagnostou, E., and Foster, G.L. 2016. An improved boron isotope pH proxy calibration for the deep-sea coral *Desmophyllum dianthus* through sub-sampling of fibrous aragonite. *Chemical Geology* **447**, 148–160.

Stumpp, M., Hu, M.Y., Melzner, F., Gutowska, M.A., Dorey, N., Himmerkus, N., Holtmann, W.C., Dupont, S.T., Thorndyke, M.C., and Bleich, M. 2012. Acidified seawater impacts sea urchin larvae pH regulatory systems relevant for calcification. *Proceedings of the National Academy of Sciences* **109**, 18192–18197.

Suzuki, M., Iwashima, A., Tsutsui, N., Ohira, T., Kogure, T., and Nagasawa, H. 2011. Identification and characterisation of a calcium carbonate-binding protein, blue mussel shell protein (BMSP), from the nacreous layer. *Chembiochem* **12**, 2478–2487.

Suzuki, M., Murayama, E., Inoue, H., Ozaki, N., Tohse, H., Kogure, T., and Nagasawa, H. 2004. Characterization of Prismalin-14, a novel matrix protein from the prismatic layer of the Japanese pearl oyster (*Pinctada fucata*). *Biochemical Journal* **382**, 205–213.

Suzuki, M., and Nagasawa, H. 2013. Mollusk shell structures and their formation mechanism. *Canadian Journal of Zoology* **91**, 349–366.

Suzuki, M., Sakuda, S., and Nagasawa, H. 2007. Identification of chitin in the prismatic layer of the shell and a chitin synthase gene from the Japanese pearl oyster, *Pinctada fucata*. *Bioscience, Biotechnology, and Biochemistry* **71**, 1735–1744.

Suzuki, M., Saruwatari, K., Kogure, T., Yamamoto, Y., Nishimura, T., Kato, T., and Nagasawa, H. 2009. An acidic matrix protein, Pif, is a key macromolecule for nacre formation. *Science* **325**, 1388–1390.

Takeuchi, T., Kawashima, T., Koyanagi, R., Gyoja, F., Tanaka, M., Ikuta, T., Shoguchi, E., Fujiwara, M., Shinzato, C., and Hisata, K. 2012. Draft genome of the pearl oyster *Pinctada fucata*: a platform for understanding bivalve biology. *DNA Research* **19**(2), 117–130. doi: 10.1093/dnares/dss005.

Tambutté, E., Tambutté, S., Segonds, N., Zoccola, D., Venn, A., Erez, J., and Allemand, D. 2012. Calcein labelling and electrophysiology: insights on coral tissue permeability and calcification. *Proceedings of the Royal Society B: Biological Sciences* **279**, 19–27.

Tambutté, E., Venn, A.A., Holcomb, M., Segonds, N., Techer, N., Zoccola, D., Allemand, D., and Tambutté, S. 2015. Morphological plasticity of the coral skeleton under CO_2-driven seawater acidification. *Nature Communications* **6**, 7368. doi: 10.1038/ncomms8368.

Taylor, J.R.A., Gilleard, J.M., Allen, M.C., and Deheyn, D.D. 2015. Effects of CO_2-induced pH reduction on the exoskeleton structure and biophotonic properties of the shrimp Lysmata californica. *Scientific Reports* **5**, 10608. doi: 10.1038/srep10608.

Taylor, P.D., Tan A.S.H., Kudryavstev, A.B., and Schopf, J.W. 2016. Carbonate mineralogy of a tropical bryozoan biota and its vulnerability to ocean acidification. *Marine Biology Research* **12**, 776–780.

ter Kuile, B., Erez, J., and Padan, E. 1989. Mechanisms for the uptake of inorganic carbon by two species of symbiont-bearing foraminifera. *Marine Biology* **103**, 241–251.

Thompson, R.F., Walker, M., Siebert, C.A., Muench, S.P., and Ranson, N.A. 2016. An introduction to sample preparation and imaging by cryo-electron microscopy for structural biology. *Methods* **100**, 3–15.

Thor, P., and Dupont, S. 2015. Transgenerational effects alleviate severe fecundity loss during ocean acidification in a ubiquitous planktonic copepod. *Global Change Biology* **21**, 2261–2271.

Titze, B., and Genoud, C. 2016. Volume scanning electron microscopy for imaging biological ultrastructure. *Biology of the Cell* **108**, 307–323.

Todgham, A.E., and Hofmann, G.E. 2009. Transcriptomic response of sea urchin larvae Strongylocentrotus purpuratus to CO_2-driven seawater acidification. *Journal of Experimental Biology* **212**, 2579–2594.

Toyofuku, T., Matsuo, M.Y., De Nooijer, L.J., Nagai, Y., Kawada, S., Fujita, K., Reichart, G.J., Nomaki, H., Tsuchiya, M., and Sakaguchi, H. 2017. Proton pumping accompanies calcification in foraminifera. *Nature Communications* **8**, 14145. doi: 10.1038/ncomms14145.

Venn, A., Tambutté, E., Holcomb, M., Allemand, D., and Tambutté, S. 2011. Live tissue imaging shows reef corals elevate pH under their calcifying tissue relative to seawater. *PLOS ONE* **6**, e20013. doi: 10.1371/journal.pone.0020013.

Venn, A.A., Tambutté, E., Holcomb, M., Laurent, J., Allemand, D., and Tambutté, S. 2013. Impact of seawater acidification on pH at the tissue–skeleton interface and calcification in reef corals. *Proceedings of the National Academy of Sciences* **110**, 1634–1639.

Vézina, A.F., and Hoegh-Guldberg, O. 2008. Introduction: effects of ocean acidification on marine ecosystems. *Marine Ecology Progress Series* **373**, 199–201.

Von Euw, S., Zhang, Q., Manichev, V., Murali, N., Gross, J., Feldman, L.C., Gustafsson, T., Flach, C., Mendelsohn, R., and Falkowski, P.G. 2017. Biological control of aragonite formation in stony corals. *Science* **356**, 933–938.

Wall, M., Fietzke, J., Schmidt, G.M., Fink, A., Hofmann, L.C., de Beer, D., and Fabricius, K.E. 2016. Internal pH regulation facilitates in situ long-term acclimation of massive corals to end-of-century carbon dioxide conditions. *Scientific Reports* **6**, 30688. doi: 10.1038/srep30688.

Wang, X., Wang, M., Xu, J., Jia, Z., Liu, Z., Wang, L., and Song, L. 2017. Soluble adenylyl cyclase mediates mitochondrial pathway of apoptosis and ATP metabolism in oyster *Crassostrea gigas* exposed to elevated CO_2. *Fish & Shellfish Immunology* **66**, 140–147.

Watabe, N. 1965. Studies on shell formation: XI. Crystal—matrix relationships in the inner layers of mollusk shells. *Journal of Ultrastructure Research* **12**, 351–370.

Wehrmeister, U., Jacob, D.E., Soldati, A.L., Loges, N., Häger, T., and Hofmeister, W. 2011. Amorphous, nanocrystalline and crystalline calcium carbonates in biological materials. *Journal of Raman Spectroscopy* **42**, 926–935.

Wei, L., Wang, Q., Wu, H., Ji, C., and Zhao, J. 2015. Proteomic and metabolomic responses of Pacific oyster Crassostrea gigas to elevated pCO_2 exposure. *Journal of Proteomics* **112**, 83–94.

Weiner, S., and Dove, P.M. 2003. An overview of biomineralization processes and the problem of the vital effect. *Reviews in Mineralogy and Geochemistry* **54**, 1–29.

Weiner, S., and Traub, W. 1980. X-ray diffraction study of the insoluble organic matrix of mollusk shells. *FEBS Letters* **111**, 311–316.

Weiss, I.M., and Schönitzer, V. 2006. The distribution of chitin in larval shells of the bivalve mollusk *Mytilus galloprovincialis*. *Journal of Structural Biology* **153**, 264–277.

Wiese, S., Reidegeld, K.A., Meyer, H.E., and Warscheid, B. 2007. Protein labeling by iTRAQ: a new tool for quantitative mass spectrometry in proteome research. *Proteomics* **7**, 340–350.

Wilbur, K.M. 1964. Shell formation and regeneration. In *Physiology and the Mollusca*, K.M. Wilbur and C.M. Younge, (eds). New York: Academic Press, 243–282.

Wilkinson, B.H. 1979. Biomineralization, paleoceanography, and the evolution of calcareous marine organisms. *Geology* **7**, 524–527.

Williams, P. 1985. Secondary ion mass spectrometry. *Annual Review of Materials Science* **15**, 517–548.

Wittmann, A.C., and Pörtner, H.O. 2013. Sensitivities of extant animal taxa to ocean acidification. *Nature Climate Change* **3**, 995–1001.

Wolfe, K., Smith, A.M., Trimby, P., and Byrne, M. 2013. Microstructure of the paper nautilus (Argonauta nodosa) shell and the novel application of electron backscatter diffraction (EBSD) to address effects of ocean acidification. *Marine Biology* **160**, 2271–2278.

Wood, H.L., Spicer, J.I., and Widdicombe, S. 2008. Ocean acidification may increase calcification rates, but at a cost. *Proceedings of the Royal Society B: Biological Sciences* **275**, 1767–1773.

Yokoo, N., Suzuki, M., Saruwatari, K., Aoki, H., Watanabe, K., Nagasawa, H., and Kogure, T. 2011. Microstructures of the larval shell of a pearl oyster, *Pinctada fucata*, investigated by FIB-TEM technique. *American Mineralogist* **96**, 1020–1027.

Zhang, C., and Zhang, R. 2006. Matrix proteins in the outer shells of molluscs. *Marine Biotechnology* **8**, 572–586.

Zhang, G., Fang, X., Guo, X. et al., 2012. The oyster genome reveals stress adaptation and complexity of shell formation. *Nature* **490**, 49–54.

Zhang, S., Henehan, M.J., Hull, P.M., Reid, R.P., Hardisty, D.S., Hood, A.V.S., and Planavsky, N.J. 2017. Investigating controls on boron isotope ratios in shallow marine carbonates. *Earth and Planetary Science Letters* **458**, 380–393.

Zhao, P., and Cai, W.J. 1999. pH polymeric membrane microelectrodes based on neutral carriers and their application in aquatic environments. *Anal. Chim Acta* **395**, 285–291.